ΣΥΛΛΟΓΟΣ ΕΛΛΗΝΩΝ ΣΥΓΚΟΙΝΩΝΙΟΛΟΓΩΝ

# Ενημερωτικό Δελτίο

ΤΕΥΧΟΣ 219 - ΣΕΠΤΕΜΒΡΙΟΣ - ΟΚΤΩΒΡΙΟΣ - ΝΟΕΜΒΡΙΟΣ 2021





A Discrete Differential Dynamic Programming Approach for GLOSA Systems with Stochastic Signal Switching Times

Lane changing and lane choice in an urban environment. The case of Panepistimiou avenue

2021

1991

**30 χρόνια**

πρωτοπορούμε
στην κατασκευή
ειδών σήμανσης


# ΣΗΜΑ

ΠΙΝΑΚΙΔΕΣ ΣΗΜΑΝΣΗΣ &
ΥΛΙΚΑ ΟΔΙΚΗΣ ΑΣΦΑΛΕΙΑΣ

---

**Τηλ.: 210 48 31 996 - Email: sales@shma.gr**

**www.shma.gr**

# EDITORIAL

***Δρ. Ιωάννα Παγώνη***
Ταμίας ΣΕΣ

Το 2021 βαίνει προς το τέλος του, αποτελώντας μια ακόμα χρονιά με πολλές προκλήσεις στον τομέα των μεταφορών παγκοσμίως. Στο διάστημα των τριών μηνών, που καλύπτει το παρόν τεύχος του Ενημερωτικού Δελτίου, διαδραματίστηκαν πολλά και σημαντικά γεγονότα που αφορούν στην επιστήμη του Συγκοινωνιολόγου.

Τα κυκλοφοριακά προβλήματα στο Λεκανοπέδιο της Αττικής και η επιστροφή του μέτρου του Δακτυλίου στο κέντρο της Αθήνας ανέδειξαν σημαντικά συγκοινωνιακά ζητήματα, ενώ η υιοθέτηση από τον Υπουργό Υποδομών και Μεταφορών Κ. Καραμανλή της πρότασης του ΣΕΣ για τη δημιουργία ενός ενιαίου Μητροπολιτικού Φορέα σχετικά με τις μεταφορές στην Αττική έφερε στο επίκεντρο τον Σύλλογο και τα μέλη του.

Το διάστημα 16 με 22 Σεπτεμβρίου 2021 έλαβε χώρα η «Ευρωπαϊκή Εβδομάδα Κινητικότητας 2021» στο πλαίσιο της οποίας υλοποιήθηκαν δράσεις με στόχο την προώθηση βιώσιμων τρόπων μετακίνησης και μεταφοράς στον αστικό ιστό και την ευαισθητοποίηση των πολιτών στη χρήση εναλλακτικών τρόπων μετακίνησής τους.

Τέλος, για 10η συνεχή φορά ο ΣΕΣ σε συνεργασία με το ΙΜΕΤ/ΕΚΕΤΑ διοργάνωσε το Συνέδριο για την Έρευνα στις Μεταφορές (ICTR 2021) το οποίο πραγματοποιήθηκε με μεγάλη επιτυχία στις 2-3 Σεπτεμβρίου, στη Ρόδο. Το συνέδριο είχε θέμα «Κινητικότητα του Μέλλοντος και Ανθεκτικές Μεταφορές: Ο δρόμος προς την Καινοτομία», ενώ η διοργάνωσή του ήταν υβριδική επιτρέποντας τόσο τη φυσική παρουσία των συμμετεχόντων όσο και την εξ' αποστάσεως συμμετοχή τους σε αυτό. Κατά τη διάρκεια του συνεδρίου, σε θεματικές συνεδρίες προβλήθηκαν τα σύγχρονα ερευνητικά αποτελέσματα και οι εξελίξεις της έρευνας σχετικά με τις μεταφορές.

Στο παρόν τεύχος του Ενημερωτικού Δελτίου, με χαρά φιλοξενούμε τρεις εργασίες που βραβεύτηκαν στο συνέδριο ICTR 2021 με το Βραβείο Νέου Ερευνητή «Ματθαίος Καρλαύτης» και το Βραβείο για την Καλύτερη Επιστημονική Εργασία στην Οδική Ασφάλεια. Στόχος μας είναι η προβολή και ανάδειξη του επιστημονικού έργου που συντελείται από νέους ερευνητές και ερευνήτριες στον τομέα των μεταφορών στη χώρα μας καθώς και εκτός Ελλάδος.

Κλείνοντας θα ήθελα να ευχαριστήσω θερμά όλα τα μέλη και τους φίλους του ΣΕΣ για τη στήριξή τους στον Σύλλογο και να ευχηθώ σε όλους θερμές ευχές για ένα καλύτερο 2022.

# ΠΕΡΙΕΧΟΜΕΝΑ



**ΕΝΗΜΕΡΩΤΙΚΟ ΔΕΛΤΙΟ**
ΣΥΛΛΟΓΟΥ ΕΛΛΗΝΩΝ ΣΥΓΚΟΙΝΩΝΙΟΛΟΓΩΝ
**ΚΩΔΙΚΟΣ: 013842**

**Τεύχος 219**
Σεπτέμβριος - Οκτώβριος - Νοέμβριος 2021

Το Δελτίο αποτελεί το τριμηνιαίο επίσημο έντυποτου Συλλόγου Ελλήνων Συγκοινωνιολόγων

**ΙΔΙΟΚΤΗΤΗΣ**
Σύλλογος Ελλήνων Συγκοινωνιολόγων
Πανόρμου 61 - 115 24 Αθήνα
τηλ.: 210 3640604 – fax: 210 3609220
e-mail: info@ses.gr, web:www.ses.gr

**ΕΚΔΟΣΗ – ΔΙΑΦΗΜΙΣΗ**
Ευαγγελία Λιάππη
τηλ.: 210 8646350 – κιν.: 6977 262610
e-mail: evi.liappi@gmail.com

**ΥΠΕΥΘΥΝΟΣ ΣΥΝΤΑΞΗΣ**
Ιωάννα Παγώνη

**ΥΠΕΥΘΥΝΟΣ ΣΥΜΦΩΝΑ ΜΕ ΤΟ ΝΟΜΟ**
Παναγιώτης Παπαντωνίου

**ΕΚΤΥΠΩΣΗ – ΒΙΒΛΙΟΔΕΣΙΑ**
Μπάνου Γκαμπριέλα Μαρία
Αντιγόνης 76 Αθήνα, τηλ.: 210 5151 233





Στέλνεται δωρεάν σε όλους τους συγκοινωνιολόγους.

ΤΙΜΗ ΤΕΥΧΟΥΣ: 0,01 ΕΥΡΩ

# 10ο Διεθνές Συνέδριο για την Έρευνα στις Μεταφορές (ICTR 2021)

Ο Σύλλογος Ελλήνων Συγκοινωνιολόγων (Σ.Ε.Σ.) και το Ινστιτούτο Βιώσιμης Κινητικότητας και Δικτύων Μεταφορών (IMET/ΕΚΕΤΑ) διοργάνωσαν το «**10ο Διεθνές Συνέδριο για την Έρευνα στις Μεταφορές» με κεντρικό θέμα: «Κινητικότητα του Μέλλοντος και Ανθεκτικές Μεταφορές: Ο δρόμος προς την Καινοτομία**» το οποίο διεξήχθη το διάστημα 1-3 Σεπτεμβρίου 2021 στη Ρόδο.

Η διοργάνωση του συνεδρίου ήταν υβριδική επιτρέποντας τόσο τη φυσική παρουσία των συμμετεχόντων όσο και την εξ' αποστάσεως συμμετοχή τους σε αυτό. Το Διεθνές Συνέδριο για την Έρευνα στις Μεταφορές αποτελεί εδώ και δεκαεννιά έτη θεσμό στην έρευνα στον τομέα των μεταφορών και απευθύνεται στην εγχώρια και διεθνή επιστημονική και ακαδημαϊκή κοινότητα, καθώς και στους ιδιωτικούς και δημόσιους φορείς και επιχειρήσεις που δραστηριοποιούνται στην ανάπτυξη και υλοποίηση καινοτόμων εφαρμογών στον τομέα των μεταφορών και συγκοινωνιακών υποδομών.

Κατά τη διάρκεια της τελετής έναρξης του ICTR 2021, οι σύνεδροι είχαν την ευκαιρία να ακούσουν την κεντρική ομιλία του κ. Mohamed Mezghani, Γενικού Γραμματέα της UITP. Η Αναπληρώτρια Διευθύντρια του IMET/ΕΚΕΤΑ Δρ. Γ. Αϋφαντοπούλου καλωσόρισε τους συμμετέχοντες και παρουσίασε τους στόχους του συνεδρίου. Τους συμμετέχοντες καλωσόρισαν επίσης ο επικεφαλής της επιστημονικής επιτροπής του ICTR 2021, καθηγητής Ν. Ηλιού, ο Διευθυντής του IMET/ΕΚΕΤΑ Δρ. Ε. Μπεκιάρης και ο Πρόεδρος του ΣΕΣ, Π. Παπαντωνίου.

Ο Γενικός Γραμματέας Χωροταξίας και Αστικού Περιβάλλοντος, Ευθύμιος Μπακογιάννης, προέβη σε παρέμβαση για τον ρόλο που παίζει το συνέδριο στην πολιτική μεταφορών και κινητικότητας για τη χώρα, τις περιφέρειες και τις πόλεις, ενώ ο Δήμαρχος Ρόδου, Αντώνιος Καμπουράκης, τόνισε τις δράσεις του δήμου, αλλά και το ισχυρό ενδιαφέρον για την ανάπτυξη βιώσιμης κινητικότητας στο νησί της Ρόδου.

Στο πλαίσιο του ICTR 2021, δόθηκαν τιμητικά βραβεία στον Ομότιμο Καθηγητή ΑΠΘ κ. Σπύρο Βούγια και τον Μελετητή κ. Βασίλη Ευμολπίδη για την εξαιρετική συμβολή τους στον τομέα των μεταφορών.

Στο πλαίσιο του Συνεδρίου απονεμήθηκαν βραβεία σε τέσσερις νέους ερευνητές και ερευνήτριες.

Το Βραβείο Νέου Ερευνητή «Ματθαίος Καρλαύτης» απονεμήθηκε σε δύο εργασίες ως ακολούθως:

- Στον Νέο Ερευνητή Παναγιώτη Τυπάλδο για την εργασία του με τίτλο "A Discrete Differential Dynamic Programming Approach for GLOSA Systems with Stochastic Signal Switching Times" και
- Στον Νέο Ερευνητή Jasso Espadaler Clapis για την εργασία του με τίτλο "Lane changing and lane choice modelling using data from a swarm of drones: The case of Panepistimiou avenue".

Δεδομένου του υβριδικού χαρακτήρα του Συνεδρίου, η απονομή των βραβείων στους Νέους Ερευνητές Παναγιώτη Τυπάλδο και Jasso Espadaler Clapis έγινε διαδικτυακά.

Το Βραβείο Νέου Ερευνητή «**Δημήτριος Τσαμπούλας**» απονεμήθηκε στη Νέα Ερευνήτρια Ελπίδα Ξένου για την εργασία της με τίτλο "Measuring the smartness of a city logistics system: A multi-criteria self-assessment tool and implementation guidelines".

Το Βραβείο για την Καλύτερη Επιστημονική Εργασία στην Οδική Ασφάλεια απονεμήθηκε στη Νέα Ερευνήτρια Εύα Μιχελαράκη για την εργασία της με τίτλο "Modelling the Safety Tolerance Zone: Recommendations from the i-DREAMS project".

Στο συνέδριο ICTR 21 έντονη ήταν εκπροσώπηση μελών του Διοικητικού Συμβουλίου του ΣΕΣ. Στη Ρόδο σε όλη τη διάρκεια του συνεδρίου συμμετείχαν ο Π. Παπαντωνίου, ο Θ. Τσιάνος, η Ν. Ντάσιου, η Ι. Παγώνη και η Δ. Αλεξανδροπούλου.


1


2


3


4

**1. Απονομή τιμητικού βραβείου στον Ομότιμο Καθηγητή ΑΠΘ κ. Σπύρο Βούγια 2. Απονομή τιμητικού βραβείου στον μελετητή κ. Βασίλη Ευμολπίδη 3. Απονομή βραβείου στη Νέα Ερευνήτρια Ελπίδα Ξένου 4. Απονομή βραβείου στη Νέα Ερευνήτρια Εύα Μιχελαράκη**

Για τη συγγραφή του παρόντος άρθρου, απονεμήθηκε στον Νέο Ερευνητή **Παναγιώτη Τυπάλδο** το Βραβείο Νέου Ερευνητή «Ματθαίος Καρλαύτης» κατά τη διάρκεια του 10ου Διεθνούς Συνεδρίου για την Έρευνα στις Μεταφορές (ICTR 2021)


# A Discrete Differential Dynamic Programming Approach for GLOSA Systems with Stochastic Signal Switching Times

**Panagiotis Typaldos[1], Vasileios Volakakis[1], Markos Papageorgiou[1], Ioannis Papamichail[1]**

## ABSTRACT

A stochastic optimal control problem was recently proposed to address the GLOSA (Green Light Optimal Speed Advisory) problem in cases where the next switching time is decided in real time and is therefore uncertain in advance. The corresponding numerical solution via SDP (Stochastic Dynamic Programming) calls for substantial computational time, which excludes problem solution in the vehicle's computer in real time. This work considers the same stochastic problem of optimal trajectory specification for vehicles approaching a signalized junction with traffic signals operating in real-time (adaptive) mode, due to which the next switching time is stochastic. However, a modified version of Dynamic Programming, known as Discrete Differential Dynamic Programming (DDDP), is used for numerical solution of the stochastic optimal control problem. It is demonstrated that the DDDP algorithm achieves results equivalent to those obtained with the ordinary SDP algorithm, albeit with significantly better performance in terms of computational time.

***Keywords:*** *GLOSA, Stochastic Dynamic Programming, Discrete Differential Dynamic Programming (DDDP), Traffic Light Advisory, Speed Advisory.*

## ΠΕΡΙΛΗΨΗ

Πρόσφατα προτάθηκε ένα πρόβλημα στοχαστικού βέλτιστου ελέγχου για το πρόβλημα GLOSA (Green Light Optimal Speed Advisory) σε περιπτώσεις όπου ο χρόνος της επόμενης εναλλαγής σήματος αποφασίζεται σε πραγματικό χρόνο και επομένως είναι αβέβαιος εκ των προτέρων. Η αντίστοιχη αριθμητική λύση μέσω ΣΔΠ (Στοχαστικού Δυναμικού Προγραμματισμού) απαιτεί αυξημένο υπολογιστικό χρόνο, ο οποίος αποκλείει τη λύση του προβλήματος στον υπολογιστή του οχήματος σε πραγματικό χρόνο. Στη παρούσα εργασία εξετάζεται το ίδιο στοχαστικό πρόβλημα προσδιορισμού βέλτιστης τροχιάς για οχήματα που προσεγγίζουν μια σηματοδοτημένη διασταύρωση με σήματα κυκλοφορίας που λειτουργούν σε πραγματικό χρόνο, που σημαίνει ότι ο επόμενος χρόνος εναλλαγής είναι στοχαστικός. Ωστόσο, μια τροποποιημένη εκδοχή του Δυναμικού Προγραμματισμού, γνωστή

ως Διακριτικός Διαφορικός Δυναμικός Προγραμματισμός (ΔΔΔΠ), χρησιμοποιείται για την αριθμητική επίλυση του στοχαστικού προβλήματος βέλτιστου ελέγχου. Διαπιστώνεται ότι ο αλγόριθμος ΔΔΔΠ επιτυγχάνει αποτελέσματα ισοδύναμα με εκείνα που λαμβάνονται με τον κλασικό αλγόριθμο ΣΔΠ, αλλά με σημαντικά καλύτερη απόδοση όσον αφορά τον υπολογιστικό χρόνο.

***Λέξεις-κλειδιά:*** *GLOSA, Στοχαστικός Δυναμικός Προγραμματισμός, Διακριτός Διαφορικός Δυναμικός Προγραμματισμός (ΔΔΔΠ), Υπόδειξη Φωτεινού Σηματοδότη, Υπόδειξη Ταχύτητας.*

# 1. INTRODUCTION

In view of cheap energy resources shortage and excessive environmental pollution, it is essential for transportation systems to operate with increased fuel efficiency. In the case of road vehicles, fuel efficiency relates to economic aspects, as fuel economy means fewer expenses for the driver; but also, to the protection of the environment in an era of climate crisis. To this end, considerable efforts in the development and deployment of efficient intelligent transportation systems (including real-time traffic signals) lead to reduced congestion and fuel consumption.

Traffic signals guarantee, in the first place, the safe crossing of vehicles at urban junctions in cities around the world. Clearly, enforcing safety via traffic lights implies that some vehicles will have to stop in front of a red light and then accelerate after the traffic light switching to green, something that affects the fuel consumption of concerned vehicles. To reduce the resulting vehicle delays and number of stops, several algorithms have been proposed and deployed over the past decades, aiming at optimizing the traffic signals operation (Hounsell and Mc-Donald, 2001; Papageorgiou et al., 2003). In fact, fuel consumption is increasingly considered as an optimization or evaluation criterion while developing and deploying signal control systems (Jamshidnejad et al., 2017).

Fixed-time signal plans are derived offline for respective times of day (e.g., morning peak period, off-peak period, etc.) by use of appropriate optimization tools, based on historical constant demands; and are applied without deviations. This implies that switching times of the traffic lights are always known in advance.

In contrast, real-time (or traffic-responsive or adaptive) signal control strategies make use of real-time measurements to calculate in real time suitable signal settings. Depending on the employed signal control strategy, the control update period may range from one second to one signal cycle. Clearly, for real-time signals, the next switching time is not known before the switching decision has been actually made.

Consider a vehicle approaching a red traffic light at a given speed. A common dilemma is whether it should maintain its speed, at the risk of having to stop if the traffic light is still red at arrival; or whether it should decelerate, as long as the traffic light is red, at some uncertain pace. This dilemma of vehicle movement when facing a red traffic signal may be addressed by appropriately designed systems. With recent and emerging advances in vehicle communications, the current state and timing of a traffic signal can be transmitted to equipped vehicles (or apps therein) to enable sensible approaching speed decisions. Based on this information, it is possible to guide the driver (or an automated vehicle) all the way to the traffic light by giving speed advice, which ensures that the vehicle will cross the traffic signal at green and with minimum fuel consumption and emissions. Systems (or apps) optimizing the vehicle approach to traffic lights are often referred to as Green Light Optimal Speed Advisory (GLOSA) systems (Stahlmann et al., 2016).

In the case of fixed signals and hence prior knowledge of the next switching time, a corresponding message is broadcasted by the signal controller. Under these conditions, the problem of how to optimize the approach to traffic signals has been addressed in different ways. Rule-based algorithms have been proposed in various works to produce advisory speeds for vehicles approaching traffic signals, so as to reduce fuel consumption and emissions (Katsaros et al., 2011; Sanchez et al., 2006; Ma et al., 2018). Optimal control approaches, considering explicitly the vehicle kinematics, are, by their nature, more pertinent in producing fuel-optimal speed profiles (Lawitzky et al., 2013; Typaldos et al., 2020a).

The situation becomes more complicated when real-time signals with very short (e.g., second-by-second) control update periods are present, in which case exact prior knowledge of the next switching time is not available. In this case, the best available knowledge can be presented as an estimate (Koukoumidis et al., 2011) or as a probabilistic distribution for the next switching time within a short-term future time-window; such a distribution may be obtained by use of statistics from previous signal operation (Mahler and Vahidi, 2012; Lawitzky et al., 2013).

In (Typaldos et al., 2020a), the problem of producing fuel-optimal vehicle trajectories for a vehicle approaching a traffic signal for both cases of known and stochastic switching times was considered. For the first case, the problem was formulated as an optimal control problem and was solved analytically via PMP (Pontryagin's Maximum Principle). Subsequently, the case of stochastic switching time with known probability distribution was also addressed, and the problem was cast in the format of a stochastic optimal control problem, which was solved numerically using SDP (Stochastic Dynamic Programming). The proposed SDP algorithm may take several minutes to execute, which implies that the solution is not real-time feasible and can therefore not be obtained on-board the vehicle, but must be executed offline, at the infrastructure side, and be communicated to approaching vehicles according to their current state.

To substantially reduce the computation time and memory requirements for the solution of the above-mentioned stochastic GLOSA problem and enable its solution onboard the vehicle, a Discrete Differential Dynamic Programming (DDDP) algorithm is employed in the current work. DDDP was proposed by Heidari (Heidari et al., 1971) for deterministic problems in the context of water resources system optimization and has been widely used in that domain to reduce the computational requirements compared with the standard DP (Dynamic Programming) algorithm of Bellman

(Bellman, 2015). DDDP is an iterative algorithm, whereby each iteration receives a feasible (but non-optimal) solution trajectory and transforms it to an enhanced one, to be used in the next iteration. The procedure starts, at the first iteration, with a feasible starting trajectory provided by the user. Each iteration employs the conventional DP algorithm to solve the problem within a strongly reduced state domain (compared to the original problem's state domain) around the received state trajectory of the previous iteration. The procedure stops, when, at some iteration, the received trajectory is found to be the optimal one, hence it cannot be further enhanced. It is also possible to reduce the discretization intervals, while advancing with the iterations, in order to improve the solution accuracy. The computational time required for each iteration is far lower compared to that of the one-shot full problem solution due to the strongly reduced space domain considered. Thus, even though we have multiple successive iterations, the computational time for all of them may still be significantly lower than for the one-shot full problem solution.

It should be noted that, in contrast to deterministic optimal control problems, stochastic optimal control problems do not feature a solution trajectory, even for given initial states, due to the uncertainty of system evolution created by the stochastic variables. However, in the specific stochastic problem (stochastic GLOSA) considered here, such a trajectory is indeed present in the problem solution, and this allows for application of the DDDP algorithm despite the stochastic nature of the problem.

The remainder of the paper is organized as follows: in Section 2, the optimal control problems with known signal switching time and uncertain signal switching time, as proposed by Typaldos et al. (2020a), are briefly presented for completeness, followed by the presentation of the DDDP algorithm. Demonstration results of the DDDP algorithms performance and comparison with the one-shot stochastic GLOSA results, are presented in Section 3. Finally, Section 4 concludes this work, summarizing its contributions and future work.

# 2. OPTIMAL CONTROL PROBLEMS AND SOLUTIONS FOR GLOSA WITH KNOWN OR UNKNOWN SIGNAL SWITCHING TIME

This section describes briefly the GLOSA approaches for the cases of known or unknown signal switching time, as proposed by Typaldos et al. (2020a); followed by the description of the DDDP approach proposed in this paper.

## 2.1 Known Signal Switching Time

Consider a vehicle traveling from an initial state $\boldsymbol{x}_0=[x_0,v_0]^T$, with $x_0$ being a given initial position and $v_0$ a given initial speed of the vehicle; with the purpose to reach a fixed final state $\boldsymbol{x}_e=[x_e, v_e]^T$ within a free (but weighted) time horizon $t_e$, with $x_e$ and $v_e$ being the vehicle's final position and speed, respectively. Between the initial and final positions, there is a traffic signal, and hence the additional restriction that the vehicle cannot pass through the traffic signal's position $x_1$ before the known time $t_1$, which is the time that the traffic light turns green from red. The implicit assumption here is that a red light is active when the vehicle appears on the link (at time 0), but a generalization, which includes the case where the vehicle appears when the traffic light is green, is given in (Typaldos et al., 2020a). The objective of the vehicle is to appropriately adjust its acceleration (control variable), so as to minimize fuel consumption, while satisfying the initial and final conditions $\boldsymbol{x}_0$ and $\boldsymbol{x}_e$, as well as the intermediate (traffic signal) constraint.

The minimization problem outlined above is formulated as an optimal control problem, which accounts for the vehicle kinematics via the following state equations:

$$\dot{x} = v \quad (1)$$

$$\dot{v} = a \quad (2)$$

where $a$ is the vehicle acceleration which assumes the role of the control variable. The objective criterion to be minimized reads

$$J = w \cdot t_e + \frac{1}{2}\int_0^{t_e} a^2\, dt \quad (3)$$

In addition, the green-light constraint, $t_S>t_1$, must be fulfilled, where $t_S$ is the time at which the vehicle crosses from the signal position $x_1$, that is, $x(t_S)=x_1$. Note that the utilized acceleration cost term $a^2$ in the cost criterion was demonstrated in an earlier study to be an excellent proxy for deriving fuel-minimizing vehicle trajectories (Typaldos et al., 2020b). Note also that the final time $t_e$ is free, but penalized with the parameter $w$. For higher values of $w$, the resulting $t_e$ will be lower and vice versa. This, consequently, affects the acceleration cost, which, depending on higher or lower $w$ value, will also have increased or decreased values (for more details see (Typaldos et al., 2020a)). If necessary, upper and lower bounds may be applied to speed $v$ and acceleration $a$.

The solution of this problem was addressed in (Typaldos et al., 2020a) and can be obtained analytically using symbolic differentiation tools. Thus, the numerical solution of the deterministic GLOSA problem, for a specific problem instance, takes only fractions of a second of computation time and can be executed in real time on-board for each approaching vehicle.

For a given junction, the final state is the same for any initial vehicle state $x_0$ and any switching time $t_1$. Therefore, the optimal value of criterion (3) of the deterministic GLOSA problem depends on these variables and is denoted $J^*_{DG}(\boldsymbol{x}_0, t_1)$ for later use.

## 2.2 Uncertain Signal Switching Time Problem

The traffic light switching time may be subject to short-term decisions in dependence of the prevailing traffic conditions in cases of real-time signals. In such cases, we typically have minimum and maximum admissible switching times; hence, based on statistics from past signal switching activity, we may derive a probability distribution of switching times within the admissible time-window of possible signal switching times. Thus, the problem can be cast in the format of a stochastic optimal control problem, which may be solved numerically using SDP techniques. To this end, the analytical solution of the deterministic GLOSA optimal control problem is used within the stochastic approach, as will be explained in this section

(for more details see (Typaldos et al., 2020a)).

For the SDP algorithm (Bertsekas, 1995), the discrete-time version of the vehicle kinematics, with time step $T$, is considered, as follows:

$$x(k+1) = x(k) + v(k)T + \frac{1}{2}a(k)T^2 \quad (4)$$

$$v(k+1) = v(k) + a(k)T \quad (5)$$

where $x(k)$, $v(k)$ correspond to the vehicle position and speed at discrete times $k = 0,1,\ldots$ (where $kT = t$), while the control variable $a(k)$ reflects the acceleration that remains constant over each time period $k$. The state and control variables are bounded within the following feasible regions

$$\boldsymbol{x}(k) \in \boldsymbol{X} = [\boldsymbol{x}_{min}, \boldsymbol{x}_{max}] \quad (6)$$

$$a(k) \in U = [a_{min}, a_{max}] \quad (7)$$

with $\boldsymbol{x}_{min}$, $\boldsymbol{x}_{max}$ and $a_{min}$, $a_{max}$ being the lower and upper bounds of the states and acceleration, respectively. The traffic light's discrete switching time $k_1$ is not known, but it is assumed that a known range $k_{min} \le k_1 \le k_{max}$ of possible switching times exists, with $k_{min}$ and $k_{max}$ being the minimum and maximum possible switching times.

For proper problem formulation, a virtual state $\tilde{x}$ (k) is introduced, that reflects formally the stochasticity of traffic light switching

$$\tilde{x}(k+1) = \tilde{x}(k) \cdot z(k), \quad \tilde{x}(0) = 1 \quad (8)$$

where $z(k)$ is a binary stochastic variable defined as

$$z(k) = \begin{cases} 0 & \text{if traffic light switches at time } k+1 \\ 1 & \text{else} \end{cases} \quad (9)$$

with (8) and (9), the virtual state $\tilde{x}$(k) is either equal to 1, if the traffic light has not yet switched until time $k$-1; or equal to 0 if switching occurred at time $k$ or earlier. The virtual state $\tilde{x}(k)$ is assumed measurable, which means that the system knows at each time $kT$ if switching has taken place or not within the last time period $[(k\text{-}1)T, kT]$.

The stochastic variable $z(k)$ is independent of its previous values and takes values according to a time-dependent probability distribution $p(z|k)$. Based on the statistics of previous signal switching activity, availability of an a-priori discrete probability distribution $P(k)$, $k_{min} \le k_1 \le k_{max}$ is assumed, for signal switching within the time-window, where $\sum_{k=k_{min}}^{k_{max}} P(k) =$

1. Since no switching takes place for $k \le k_{min}$-1, we have

$$p(0 \mid k) = 0 \quad \text{for} \quad k < k_{min}\text{-}1 \quad (10)$$

For $k \ge k_{min}$, the probability distribution $p(z|k)$, is obtained by use of "crop-and-scale", meaning that the a-priori probabilities of previous time steps, where switching did not take place, are distributed analogously to increase the probabilities of the remaining discrete times within the time-window (Lawitzky et al., 2013). As shown by Typaldos et al. (2020a), this update may be done by use of the following crop-and-scale formula that applies for $k_{min} \le k \le k_{max}$-1 and for any a-priori distribution $P(k)$

$$p(0|k) = \frac{P(k+1)}{\sum_{\kappa=k+1}^{k_{max}} P(\kappa)} \quad (11)$$

where the term in brackets reflects the crop-and-scale update.

The cost criterion of the stochastic problem is the same as in the deterministic case (3). However, in the stochastic case, the exact value of the criterion depends on the stochastic variable's realization, and therefore we consider minimization of the expected value

$$J = E\left\{w \cdot t_e + \frac{1}{2}\int_0^{t_e} a^2\, dt\right\} \quad (12)$$

where the expectation refers to the stochastic variable $z(k)$, $k=0,\ldots,$ $k_{max}$-1. Note that, when the switching time becomes known at time $k_1$, while the vehicle is at state $\boldsymbol{x}(k_1)$, the problem instantly becomes a deterministic GLOSA problem, and the corresponding optimal cost-to-go is $J^*_{DG}[\boldsymbol{x}(k_1), k_1]$, which will be denoted as the "escape cost".

To obtain a formally proper cost criterion, the stochastic variable $z(k)$ and the virtual variable $\tilde{x}(k)$ introduced earlier are used, and, as shown by Typaldos et al. (2020a), this yields the objective function in the required form, as follows

$$J = E\left\{\tilde{x}(k) \sum_{k=0}^{k_{max}-1} \left[\frac{1}{2}a(k)^2 + [1 - z(k)] \cdot J^*_{DG}[\boldsymbol{x}(k), a(k), k+1]\right]\right\} \quad (13)$$

Equations (4)-(13) constitute an ordinary stochastic optimal control problem (Bertsekas, 1995). Denoting the corresponding optimal cost-to-go function by $V[\boldsymbol{x}(k), \tilde{\boldsymbol{x}}(k), k]$, the recursive Bellman equation for $0 \le k \le k_{max}$-1 reads

$$\begin{aligned} V[\boldsymbol{x}(k), \tilde{x}(k), k] = \\ = \min_{a(k)\in U}\left\{E\left\{\frac{1}{2}a(k)^2 + [1 - z(k)] \cdot J^*_{DG}[\boldsymbol{x}(k), a(k), k+1]\right.\right. \\ \left.\left. + V[\boldsymbol{x}(k+1), \tilde{x}(k)z(k), k+1]\right\}\right\} \\ = \min_{a(k)\in U}\left\{\frac{1}{2}a(k)^2 + p(0|k) \cdot J^*_{DG}[\boldsymbol{x}(k), a(k), k+1] + [1 - p(0|k)]\right. \\ \left. \cdot V[\boldsymbol{x}(k+1), 1, k+1]\right\} \end{aligned} \quad (14)$$

with boundary condition $V[\boldsymbol{x}(k_{max}), 1, k_{max}] = 0$.

## 2.3 Discrete SDP Numerical Solution Algorithm

For the numerical solution of the stochastic problem, using the SDP algorithm, the state and control variables must be discretized. As the discretization level has a significant impact on computational time and memory requirements, but also on the accuracy of the computed solution, an appropriate trade-off should be specified between reasonable computation requirements versus achievable solution quality.

For the discretization, the discrete time interval, $T$ is set equal to 1 s, which is a reasonable choice for the problem at hand. Then, a general discretization interval $\Delta$ for the problem variables is assumed, and the discretization interval of acceleration is set $\Delta a = \Delta$. From (5), the discretization interval of speed assumes the same value ($\Delta v = \Delta a = \Delta$). Likewise, in view of (4), the discretization interval for the position is

$$\Delta x = \frac{1}{2}\Delta \cdot T^2 \quad (15)$$

Based on these settings, it was shown in (Typaldos et al., 2020a) that, if $x(k)$, $v(k)$, $a(k)$ are discrete points, then $x(k+1)$ and $v(k+1)$

resulting from (4) and (5) are also discrete points.

It is now straightforward to apply the discrete SDP algorithm to obtain an optimal closed-loop control law $a(k)^*=R[\boldsymbol{x}(k), k]$, which for any given vehicle state $\boldsymbol{x}(k)\in\boldsymbol{X}$ and time $k$, delivers the optimal acceleration $a(k)^*$. The SDP algorithmic steps are summarized below. Note that the algorithm needs to consider only the case $\bar{x}(k)=1$, therefore any arguments pertaining to $\bar{x}(k)$ are suppressed for convenience.

The SDP algorithm is described as follows:

$V[\boldsymbol{x}(k_{max}), k_{max})\,] \leftarrow 0 \quad \forall\, \boldsymbol{x}(k_{max}) \in \boldsymbol{X}$
**for** each $k = k_{max} - 1, \ldots, 0$ **do**
  **for** each discrete state $x(k) \in \boldsymbol{X}$ **do**
    **for** each discrete control $a(k) \in U$ **do**
      Calculate $x(k+1), v(k+1)$
      **if** $\boldsymbol{x}(k+1) \notin \boldsymbol{X}$ **then**
        $J[\boldsymbol{x}(k), a(k), k] \leftarrow \infty$
        **continue**
      **end if**
      $J[\boldsymbol{x}(k), a(k), k]$
        $\leftarrow \frac{1}{2}\, a(k)^2 + p(0|k) \cdot J^*_{[DG]}[\boldsymbol{x}(k), a(k), k]$
        $+ [1 - p(0|k)] \cdot V[\boldsymbol{x}(k+1), k+1]$
    **end for**
    $V[\boldsymbol{x}(k), k] \leftarrow \min J[\boldsymbol{x}(k), a(k), k] \quad \forall\, a(k) \in U$
    $R[\boldsymbol{x}(k), k] = a(k)^* \leftarrow \arg \min_{a(k)\in U} J[\boldsymbol{x}(k), a(k), k]$,
    with $a(k)^*$ the optimal control of point $[\boldsymbol{x}(k), k]$
  **end for**
**end for**

As mentioned, this algorithm delivers an optimal control law $a(k)^*=R[\boldsymbol{x}(k),k]$ for the full state domain $\boldsymbol{X}$. Note that general stochastic optimal control problems do not possess a solution trajectory for specific initial states $\boldsymbol{x}_0$, because the state evolution is uncertain in presence of the stochastic variables. However, in the specific GLOSA problem addressed here, the evolution of the vehicle state (4), (5) is not affected by the stochastic variable $z(k)$, which concerns only the signal switching time. Thus, for a given initial state, i.e. vehicle position and speed at time 0, the optimal control law may be used to produce an optimal vehicle trajectory that the vehicle should pursue; until the signal switching actually occurs, in which case the vehicle should instantly behave according to the deterministic GLOSA solution.

### 2.4 Discrete Differential Dynamic Programming

The major disadvantage of the discrete (S)DP algorithm is the high computation time required for the numerical solution of the optimal control problem. To address this weakness, several modified DP algorithms have been proposed, which lead to reduction of the computational effort; and one of them is the DDDP algorithm, proposed in (Heidari et al., 1971) for deterministic optimal control problems. The method can nevertheless be applied here, because an optimal vehicle trajectory may be derived for the stochastic GLOSA problem, despite its stochastic character.

As already mentioned, DDDP is an iterative algorithm, calling for a feasible starting state trajectory to be specified externally. Each iteration $l$ receives a feasible (but non-optimal) state trajectory $\boldsymbol{x}^{(l-1)}(k)$, and transforms it to an enhanced one $\boldsymbol{x}^{(l)}(k)$, to be used in the next iteration. To this end, each iteration solves a discrete SDP problem by use of the standard SDP algorithm presented above.

What changes at each iteration $l$ is the considered state domain $\boldsymbol{X}_C^{(l)} = \left\{\boldsymbol{x}(k) \mid \left|\boldsymbol{x}(k) - \boldsymbol{x}^{(l-1)}(k)\right| \le \boldsymbol{\Delta}_C^{(l)} \wedge \boldsymbol{x}(k) \in \boldsymbol{X}\right\}$, which is a strongly reduced subdomain of the original state domain $\boldsymbol{X}$ in (6). In other words, the discretized SDP problem is solved in each iteration $l$ within a corridor with width $\boldsymbol{\Delta}_C^{(l)}$, around the received state trajectory $\boldsymbol{x}^{(l-1)}(k)$ of the previous iteration, to produce a solution trajectory $\boldsymbol{x}^{(l)}(k)$ for use in the next iteration. The corridor width $\boldsymbol{\Delta}_C^{(l)}$, as well as the discretization intervals $\Delta a^{(l)}$, $\Delta x^{(l)}$, can vary in each iteration, typically at a decreasing rate. The procedure stops when a termination criterion is satisfied.

In the proposed GLOSA application, the starting trajectory for the first iteration of DDDP is the optimal solution of the deterministic GLOSA problem, assuming the "pessimistic" case where the traffic light will switch from red to green at the latest possible time, that is, at $k_1=k_{max}$, so as to cover the whole time range and be not too far from the stochastic optimal trajectory; see (Typaldos et al., 2020a). The discretization intervals $\Delta a^{(1)}$, $\Delta \boldsymbol{x}^{(1)}$ for the first iteration are also given. The intervals are reduced by half, each time there is no solution improvement at two subsequent iterations. The corridor width is taken as $\boldsymbol{\Delta}_C^{(l)} = (\boldsymbol{C} \cdot \Delta a^{(l)})$, where $\boldsymbol{C} = [C_x, C_v]$ are constant given values specifying the state corridor width. Thus, the corridor's initial width is defined through the chosen values for $\boldsymbol{C}$ and $\Delta a^{(l)}$. In the following iterations, whenever the discrete interval is reduced, there is an analogous reduction of the corridor width. Consequently, we have a constant number of feasible discrete points in all iterations, which facilitates the algorithm's fine-tuning so as to improve its computational efficiency. Note that, $C_x$ and $C_v$ values may differ, as the magnitude of the two respective state variables differs.

The admissible control region $U$ (see (7)) is kept the same at each iteration, although many related state transitions cannot be considered in view of the reduced state variables domain. The algorithm terminates whenever there is no improvement of the produced solution trajectory even after a reduction of the discretization intervals; or when the $\Delta a^{(l)}$ value becomes less than 0.125, which was found in (Typaldos et al., 2020a) to lead to sufficiently accurate results.

It should be noted that there is no general guarantee that the DDDP iterations will actually converge to the full-domain SDP solution. In particular, if the state sub-domains $\boldsymbol{X}_C^{(l)}$ considered in the iterations are too small, the obtained DDDP solution may actually differ from the SDP solution. On the other hand, if the state sub-domains are selected large, the required number of iterations may decrease, but the computation time required to find the solution at each iteration increases accordingly. In conclusion, some fine-tuning regarding the size of sub-domains is necessary to ensure convergence to the SDP solution with minimum overall (all iterations) computation time.

## 3. RESULTS

In this section, some results using the proposed DDDP approach are presented. Several scenarios have been tested, with different initial and final conditions, different switching windows and different probability distributions. In these scenarios, different

situations occur, such as cases where the vehicle needs to accelerate or decelerate before or after crossing the traffic signal; or cases where the vehicle is even forced to fully stop and wait until the traffic light's switch from red to green.

One scenario will be presented here (more results and scenarios are being considered in ongoing work) with the following initial and final conditions: $x_0 = 0$ m, $v_0 = 5$ m/s, $x_e = 220$ m, $v_e = 11$ m/s and $w = 0.1$.

The traffic light position is $x_1$=150 m. The states and control bounds are set to $[x_{min}, x_{max}]$=[0,150] m, $[v_{min}, v_{max}]$=[0,16] m/s, $[a_{min}, a_{max}]$=[-3,3] m/s$^2$, respectively. The time step $T$ is 1 s and the switching time range for the traffic light is $[k_{min}, k_{max}]$=[10,30] with uniform a-priori probability distribution. For the initial discretization, $\Delta a$=$\Delta v$=0.5 is used, which leads to $\Delta x$=0.25 m and the initial corridor width is set $\boldsymbol{C}$ = [20,4], i.e. we have $C_x$=5·$C_v$. The choice of the initial discretization and corridor width value will be justified later in this section.

Figures 1 and 2 display the optimal state (speed) and control (acceleration) trajectories over each iteration of the DDDP algorithm. Note that, position trajectories are not included, as the difference of those trajectories, at each iteration, is small and barely visible. Specifically, in each iteration we consider a corridor $\boldsymbol{\Delta}_C^{(l)} = [-\boldsymbol{C} \cdot \Delta a^{(l)}, \boldsymbol{C} \cdot \Delta a^{(l)}]$ around the respective received state trajectories, which cannot of course extend out of the full state bounds.

In both Figures 1 and 2, the dashed blue lines represent, for each iteration, the received trajectory, the solid orange lines represent the optimal trajectories derived, and the red dashed lines reflect the corresponding corridor bounds. It can be observed from Figures 1-2 that, starting with the initial chosen discretization, the first DDDP iteration improves the initial trajectory, leading to a better solution, which is optimal within the considered sub-domain. In the second iteration, no further improvement can be achieved, which means that, with the current discretization values, the best achievable solution has been reached. By reducing the discretization at the 3rd iteration, a reduction in the corridor width is observed, but the number of discrete points remains the same. This reduction enables further improvement of the solution, and the procedure continuous until the termination criterion is fulfilled. Table 1 contains the values of the objective function for each iteration of the DDDP algorithm, assuming $\Delta a$=0.5 and $\boldsymbol{C}$=[20,4], where the choice of these values will be explained in the following.

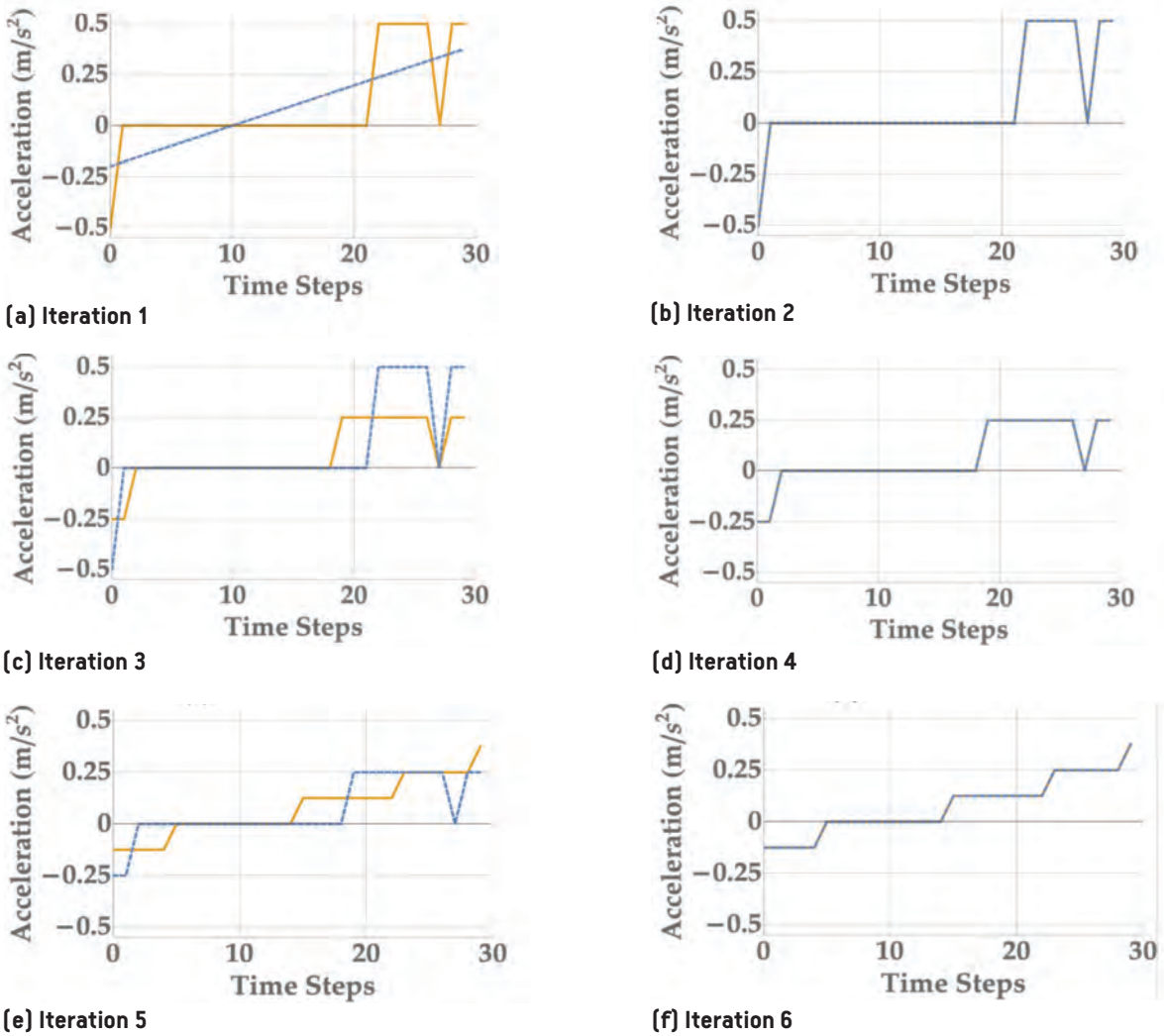


(a) Iteration 1 (b) Iteration 2

(c) Iteration 3 (d) Iteration 4

(e) Iteration 5 (f) Iteration 6

**Figure 1: Received (blue dashed line) and optimal (orange line) acceleration trajectories of DDDP algorithm in each iteration.**

In Table 2, the results of DDDP for different initial corridor C and discretization Δa values are presented. It can be seen that, for all presented discretization values, as the corridor's width is increased, a reduction of the number of DDDP iterations is observed. This behaviour is expected, as the bigger corridors, i.e. bigger admissible regions, lead to potentially better solutions at each iteration, and hence to fewer iterations to reach the original SDP problem's

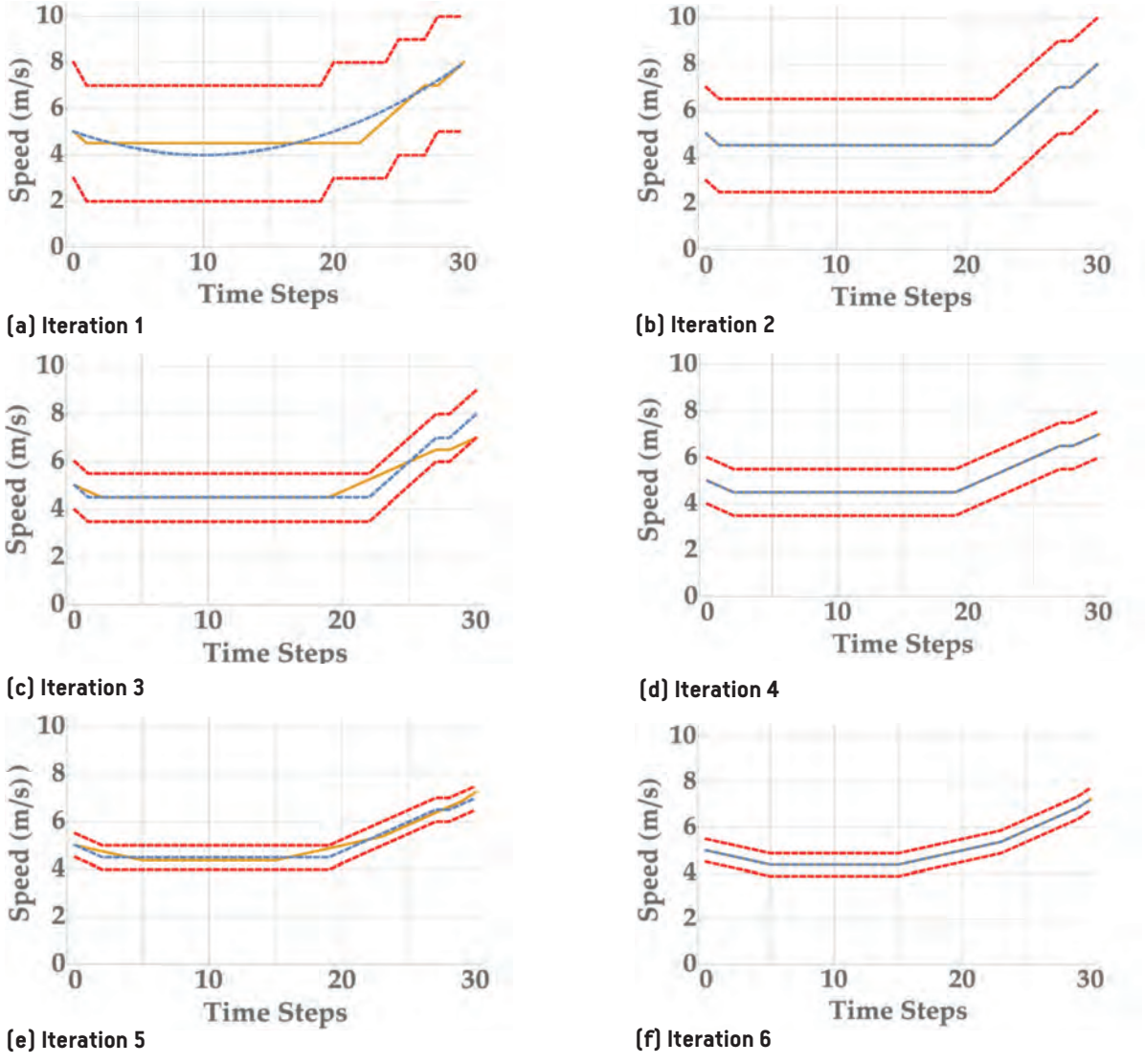


**Figure 2: Received (blue dashed line) and optimal (orange line) speed trajectories of DDDP algorithm in each iteration. The corridor $\Delta_c^{(q)}$ is marked with red dashed lines.**

optimal solution. On the other hand, despite the decrease on the number of iterations, the overall computation time is increased due to the higher computation time required at each iteration, which in turn, is due to more feasible discrete state points included. Moreover, for very small values of $C$, it is noticed that DDDP could not converge to the best possible solution when the termination criterion is fulfilled, due to the extremely limited state space.

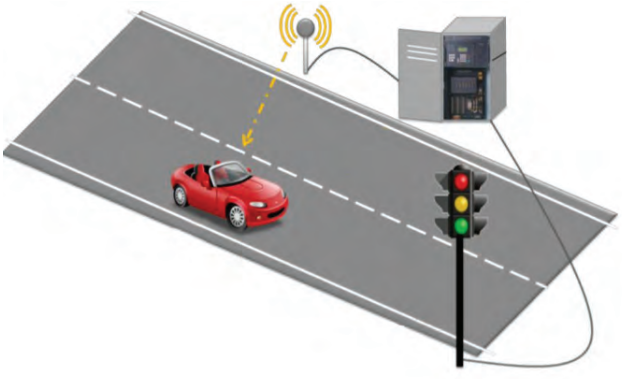

**Table 1: Optimal Cost evolution and discretization change in each iteration of DDDP algorithm**

| Iter. | $\Delta a = \Delta v$ | $\Delta x$ | Cost |
|---|---|---|---|
| 1 | 0.5 | 0.25 | 1.357 |
| 2 | 0.5 | 0.25 | 1.357 |
| 3 | 0.25 | 0.125 | 1.223 |
| 4 | 0.25 | 0.125 | 1.223 |
| 5 | 0.125 | 0.0625 | 1.175 |
| 6 | 0.125 | 0.0625 | 1.175 |

**Table 2: Performance of DDDP algorithm in terms of CPU-time and optimal cost for different initial values of $C$ and $\Delta a$**

| | $\Delta a = 1.0$ | | | $\Delta a = 0.5$ | | |
|---|---|---|---|---|---|---|
| $C_v$ | Iter. | CPU time (s) | Cost | Iter. | CPU time (s) | Cost |
| 2 | 19 | 0.648 | 1.199 | 20 | 0.612 | 1.193 |
| 3 | 19 | 1.296 | 1.177 | 8 | 0.552 | 1.175 |
| 4 | 15 | **1.655** | 1.175 | 6 | **0.692** | 1.175 |
| 5 | 12 | 1.839 | 1.175 | 6 | 1.052 | 1.175 |
| 6 | 10 | 2.298 | 1.175 | 6 | 1.451 | 1.175 |
| | $\Delta a = 0.25$ | | | $\Delta a = 0.125$ | | |
| $C_v$ | Iter. | CPU time (s) | Cost | Iter. | CPU time (s) | Cost |
| 2 | 10 | 0.326 | 1.193 | 5 | 0.280 | 1.193 |
| 3 | 6 | 0.469 | 1.179 | 5 | 0.443 | 1.179 |
| 4 | 7 | **0.867** | 1.175 | 5 | **0.762** | 1.175 |
| 5 | 6 | 1.111 | 1.175 | 4 | 0.885 | 1.175 |
| 6 | 5 | 1.291 | 1.175 | 3 | 0.967 | 1.175 |

Based on these observations, the selection of the values $C$= [20,4] and $\Delta a$=0.5 seems to be a reasonable choice, and this choice was found to lead to similar results also in several other scenarios, not presented here.

The accuracy of the DDDP algorithm compared to the full one-shot SDP solution is assessed in Figure 3. In this figure, the optimal state (speed) and control (acceleration) trajectories

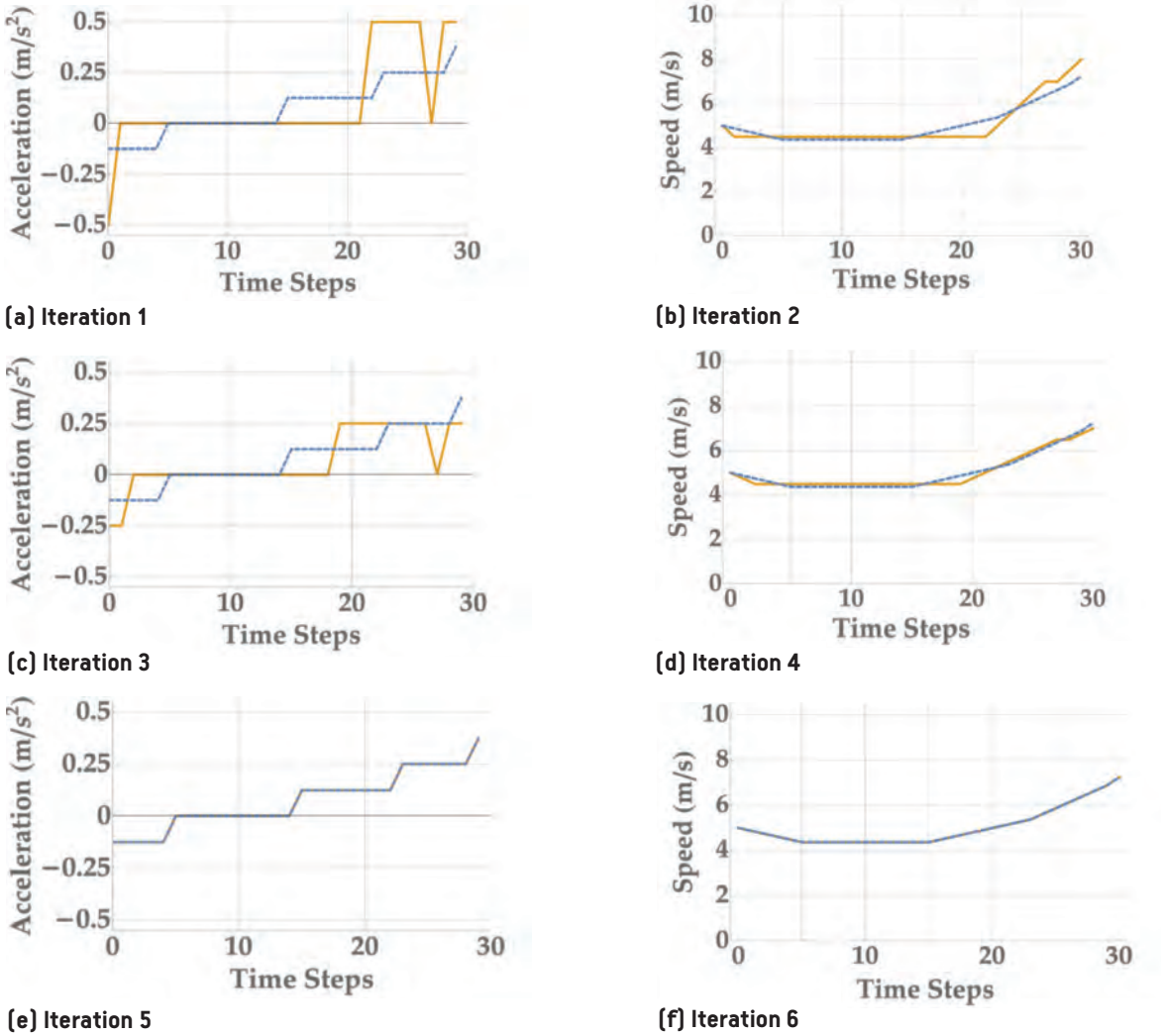


**Figure 3: Optimal acceleration and speed trajectories (orange line) of three DDDP iterations, compared with corresponding optimal trajectories of the one-shot SDP (blue dashed line).**

(orange lines), in the first, middle and last DDDP iterations are contrasted to the corresponding optimal trajectories derived from the full-range SDP (blue dashed lines) with a discretisation of $\Delta a$ = 0.125. It can be seen that DDDP, starting in the first iteration with the initial trajectory derived from the "pessimistic" deterministic GLOSA problem, manages to converge at the exact same optimal solution as the full-range SDP. The obtained optimal cost of both approaches is 1.17517, while the computation time difference is remarkable, as the one-shot SDP needs 613.86 s to obtain the solution, while DDDP needs only 0.69 s. More importantly, this big reduction in computation time enables the DDDP algorithm to be executable in real time, even in an MPC (Model Predictive Control) mode, on the vehicle side, similarly to the deterministic GLOSA.

## 4. CONCLUSIONS

The current work is an extension of a previous work (Typaldos et al., 2020a), where a stochastic GLOSA methodology was developed, by optimizing, using SDP techniques, the vehicle kinematic trajectories subject to the intermediate stochastic traffic signal switching constraint and with a fixed final state. In the present extension, a Discrete Differential Dynamic Programming (DDDP) algorithm was developed, which solves the original SDP problem iteratively, each time considering a reduced state space. Demonstration results demonstrate that the DDDP algorithm strongly outperforms, by a factor of 1:1000 the full-range SDP in terms of computation time. This enables the DDDP algorithm to be executable in real time on-board approaching vehicles, even in a model predictive control (MPC) mode.

Current and future work is focused on:

- Generalization of the current GLOSA problem by considering uncertain switching times for both green and red phases.
- Solving the SDP problem with a different modified iterative DP algorithm, in an attempt to further reduce the computational time.


### ACKNOWLEDGEMENTS

*The research leading to these results has received funding from the European Research Council under the European Union's Seventh Framework Programme (FP/2007-2013) / ERC Grant Agreement n. [321132], project TRAMAN21 as well as from related matching funds by the Greek Ministry of Education, Research and Religious Affairs (General Secretariat for Research and Technology).*


**4. References - Bibliography**


- Bellman, R.E. (2015). Adaptive control processes: a guided tour, volume 2045. Princeton University Press.
- Bertsekas, D.P. (1995). Dynamic programming and optimal control, volume 1. Athena scientic Belmont, MA.
- Heidari, M., Chow, V.T., Kokotovic, P.V., and Meredith, D.D. (1971). Discrete dierential dynamic programing approach to water resources systems optimization. Water Resources Research, 7(2), 273-282.
- Hounsell, N. and McDonald, M. (2001). Urban network traffic control. Proceedings of the Institution of Mechanical Engineers, Part I: Journal of Systems and Control Engineering, 215(4), 325-334.
- Jamshidnejad, A., Papamichail, I., Papageorgiou, M., and De Schutter, B. (2017). Sustainable model-predictive control in urban traffic networks: Efficient solution based on general smoothening methods. IEEE Transactions on Control Systems Technology, 26(3), 813-827.
- Katsaros, K., Kernchen, R., Dianati, M., and Rieck, D. (2011). Performance study of a green light optimized speed advisory (glosa) application using an integrated cooperative its simulation platform. In 2011 7th International Wireless Communications and Mobile Computing Conference, 918-923. IEEE.
- Koukoumidis, E., Peh, L.S., and Martonosi, M.R. (2011). Signalguru: leveraging mobile phones for collaborative traffic signal schedule advisory. In Proceedings of the 9th international conference on Mobile systems, applications, and services, 127-140.
- Lawitzky, A., Wollherr, D., and Buss, M. (2013). Energy optimal control to approach traffic lights. In 2013 IEEE/RSJ International Conference on Intelligent Robots and Systems, 4382-4387. IEEE.
- Ma, J., Zhou, F., Huang, Z., Melson, C.L., James, R., and Zhang, X. (2018). Hardware-in-the-loop testing of connected and automated vehicle applications: a use case for queue-aware signalized intersection approach and departure. Transportation Research Record, 2672(22), 36-46.
- Mahler, G. and Vahidi, A. (2012). Reducing idling at red lights based on probabilistic prediction of traffic signal timings. In 2012 American Control Conference (ACC), 6557-6562. IEEE.
- Papageorgiou, M., Diakaki, C., Dinopoulou, V., Kotsialos, A., and Wang, Y. (2003). Review of road traffic control strategies. Proceedings of the IEEE, 91(12), 2043-2067.
- Sanchez, M., Cano, J.C., and Kim, D. (2006). Predicting traffic lights to improve urban traffic fuel consumption. In 2006 6th International Conference on ITS Telecommunications, 331-336. IEEE.
- Stahlmann, R., Moller, M., Brauer, A., German, R., and Eckho, D. (2016). Technical evaluation of glosa systems and results from the field. In 2016 IEEE Vehicular Networking Conference (VNC), 1-8. IEEE.
- Typaldos, P., Kalogianni, I., Mountakis, K.S., Papamichail, I., and Papageorgiou, M. (2020a). Vehicle trajectory specification in presence of traffic lights with known or uncertain switching times. Transportation Research Record, 2674(8), 53-66.
- Typaldos, P., Papamichail, I., and Papageorgiou, M. (2020b). Minimization of fuel consumption for vehicle trajectories. IEEE Transactions on Intelligent Transportation Systems, 21(4), 1716-1727.



***Panagiotis Typaldos[1], Vasileios Volakakis[1], Markos Papageorgiou[1], Ioannis Papamichail[1]***

[1]Dynamic Systems & Simulation Laboratory
School of Production Engineering
& Management Technical University of Crete

Για τη συγγραφή του παρόντος άρθρου, απονεμήθηκε στον Νέο Ερευνητή **Jasso Espadaler Clapés** το Βραβείο Νέου Ερευνητή «Ματθαίος Καρλαύτης» κατά τη διάρκεια του 10ου Διεθνούς Συνεδρίου για την Έρευνα στις Μεταφορές (ICTR 2021)

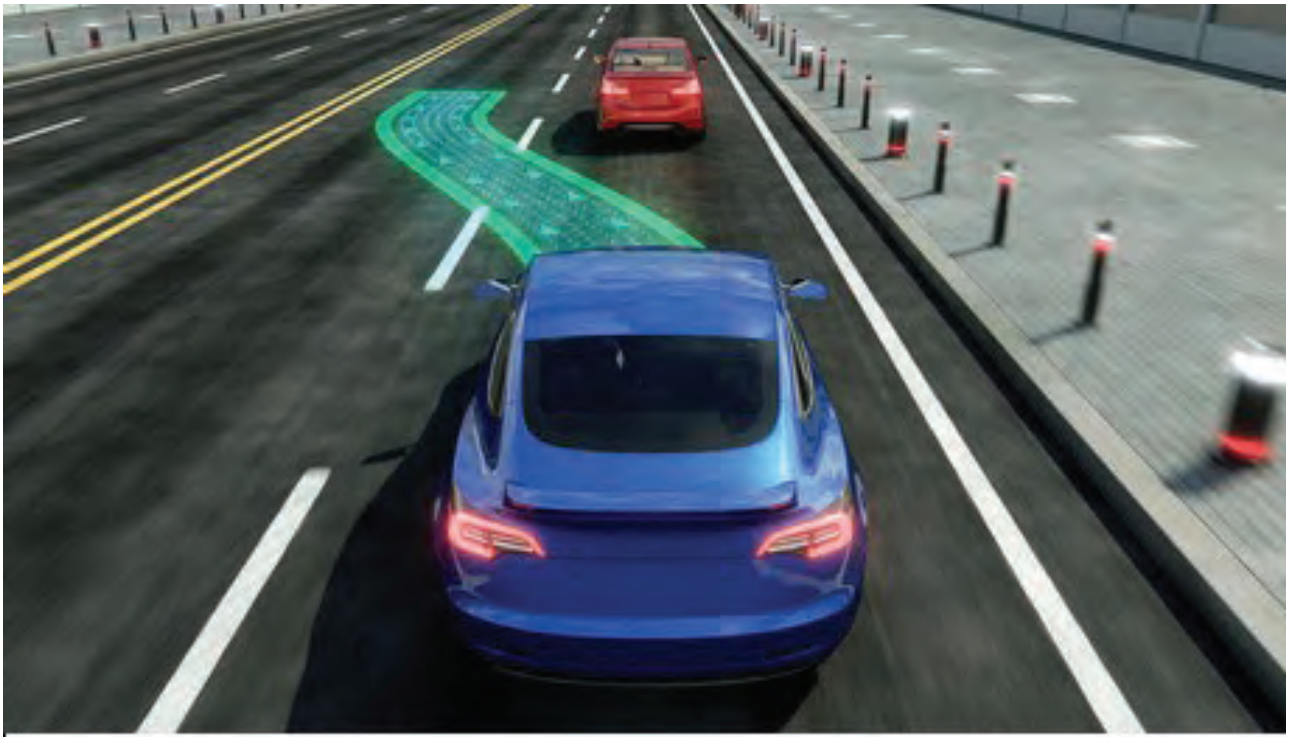

# Lane changing and lane choice in an urban environment. The case of Panepistimiou avenue

**Jasso Espadaler Clapıs[1], Emmanouil Barmpounakis[1], Nikolas Geroliminis[1]**

## ABSTRACT

The pNEUMA dataset is the result of a unique field experiment using a swarm of ten drones flying over the central district of Athens, Greece. Using this newly available dataset, this paper focuses on two directly related topics: i) lane changing and ii) lane choice in one of the busiest arterials in the city (Panepistimiou avenue). The main concept of this study relies on the definition of two layers regarding how the six lanes of the arterial are actually being used. Specifically, we argue that the lanes that are marked on the arterial (marked layer) are influenced by the frictions created by buses, bus stops, taxi stops, illegal on-street parking, etc. Using a lane detection algorithm, we show that there is an active layer which is different to the marked lanes on the road affecting capacity in the macroscopic level and driving behavior in the microscopic.

***Keywords:*** *unmanned aerial systems, swarm of drones, traffic monitoring, traffic flow modeling, multimodal systems, lane changing, lane choice.*

## ΠΕΡΙΛΗΨΗ

Η βάση δεδομένων pNEUMA είναι το αποτέλεσμα ενός μοναδικού πειράματος όπου χρησιμοποιήθηκε ένα σμήνος δέκα drones πάνω από την κεντρική περιοχή των Αθηνών. Χρησιμοποιώντας αυτά τα προσφάτως διαθέσιμα δεδομένα, αυτή η εργασία επικεντρώνεται σε δύο άμεσα σχετιζόμενα θέματα: i) αλλαγή λωρίδας και ii) επιλογή λωρίδας σε μια από τις πιο πολυσύχναστες αρτηρίες της πόλης (Λεωφόρος Πανεπιστημίου). Η βασική ιδέα αυτής της εργασίας βασίζεται στον ορισμό δύο επιπέδων σε σχέση με τον τρόπο με τον οποίο χρησιμοποιούνται οι έξι λωρίδες της αρτηρίας. Συγκεκριμένα, υποστηρίζουμε ότι οι λωρίδες που επισημαίνονται στο οδόστρωμα («μαρκαρισμένο επίπεδο») επηρεάζονται από τις αλληλεπιδράσεις που δημιουργούνται από κινήσεις λεωφορείων, στάσεις λεωφορείων, στάσεις ταξί, παράνομη στάθμευση κ.λπ. Χρησιμοποιώντας έναν αλγόριθμο ανί-

χνευσης λωρίδων, δείχνουμε ότι υπάρχει ένα άλλο επίπεδο («ενεργό επίπεδο») που διαφέρει από τις επισημασμένες λωρίδες στο δρόμο που επηρεάζουν την κυκλοφοριακή ικανότητα σε μακροσκοπικό επίπεδο και την οδηγική συμπεριφορά σε μικροσκοπικό.

***Λέξεις - κλειδιά:*** *μη επανδρωμένα εναέρια συστήματα, σμήνος drone, παρακολούθηση κυκλοφορίας, προτυποποίηση κυκλοφοριακής ροής, πολυτροπικά μεταφορικά συστήματα, αλλαγή λωρίδας, επιλογή λωρίδας.*

# 1. INTRODUCTION

Understanding how vehicles drive in an urban congested environment has drawn the attention of the transportation research community which has been craving for high-quality datasets for years. Yet, the lack of reliable data has prevented researchers from properly studying traffic phenomena in such a context. Recent progress in data collection techniques using unmanned aerial systems (UAS or commonly known as UAVs or drones) has allowed the development massive datasets to study congestion and traffic phenomena in cities.

The pNEUMA dataset (https://open-traffic.epfl.ch) is precisely the result of a unique field experiment using a swarm of ten drones flying over the central district of Athens, Greece and offers a unique opportunity to study traffic-related phenomena in a multimodal, congested and urban environment (E. Barmpounakis & Geroliminis, 2020). The authors demonstrated the convenience of drones for the collection of massive datasets with the realization of a unique experiment with ten drones in Athens, Greece. The result of this field experiment was a dataset with over 0.5 million detailed trajectories ready for use to the entire scientific community.

In order to better utilize the pNEUMA dataset, (E. Barmpounakis et al., 2020) described a methodology to extract traffic information at the lane level. The authors presented an algorithm based on the Jenks natural breaks classification method that allows to cluster the trajectories and identify the lanes from the data. Additionally, they provided another algorithm for lane-changing maneuver detection based on the concept of azimuth with both algorithms having a high accuracy over 95%. Using this newly available dataset, the current work focuses on two understudied and directly related topics: i) lane changing and ii) lane choice in urban environments.

With regards to lane changing studies, there has been an extensive research especially on the modeling in freeways. A well-known example is the MOBIL model (minimizing overall braking induced by lane changes) introduced in (Kesting et al., 2007) and applied to traffic simulation data. It is built on an acceleration function that considers the speed of the vehicle, the distance to the front vehicle and their relative speed. Additionally, it includes a politeness factor to account for driver aggressiveness. In (Toledo et al., 2003) the authors introduced an integrated lane-changing model that allows drivers to consider mandatory and discretionary lane changes at the same time with a utility function. The modeling is based on target lane choice and gap acceptance models and was validated with freeway trajectory data in the US. The study of (Toledo et al., 2005) explored the relation of lane changing models to lane choice in highways, by presenting a generalized lane-changing model in which drivers choose their lane based on a variety of reasons.

Yet, there have been some attempts to investigate how vehicles drive in an urban environment. (Gipps, 1986) proposed a first framework to understand the lane-changing decisions made by drivers in an urban driving situation. The emphasis was put in the hierarchy of decisions to produce logical and realistic traffic simulations. Another example to understand vehicle trajectory in urban arterials was given by (Wei et al., 2000). The authors proposed a lane-assignment model to describe the trajectory of a vehicle in an urban context. The model is the result of empirical observations of the lane choice from videos in eight streets in Kansas City, US. On top of the mandatory and discretionary lane changes the authors introduced the concept of preemptive lane changes, representing the lane changes towards the turning lane at a downstream intersection. On the other hand, (Choudhury & Ben-Akiva, 2008) presented a novel choice model for urban arterial intersections based on the concept of target lane, which is the lane that is better perceived to drive on. The lane selection model is shaped as a two-level decision: choice of the target lane and choice of immediate lane. The parameters were estimated with vehicle trajectories in an important intersection in Lankershim Boulevard in Los Angeles, California. Furthermore, (Sun & Elefteriadou, 2012) focused on the drivers to understand their behavior when performing a lane change in an urban context. For that purpose, they used an instrumented vehicle to observe the driver's actions, the background of the driver and the trajectory. The results allowed to classify the 40 drivers of the experiment into four big groups according to their lane-changing maneuvers. Finally, understanding lane choice and the way vehicles drive in an urban arterial is vital for future research on autonomous vehicles. An example of recent research on the matter is (Lu et al., 2020). The authors predict lane-level short-term traffic speed using a new mixed deep learning model. Speed is assumed to have a key role on lane choice -and thus lane changing-: being able to evaluate speed in the short term allows to make better decisions on the lane to drive on.

Lane-changing activity is also supposed to play a role in the capacity of a network. One of the first attempts to model lane-changing behaviors and their effects was (Laval & Daganzo, 2006). The publication is based on the idea that a vehicle changing the lane acts as moving bottleneck on the new lane. The authors used theoretical experiments to validate the model and lacks an empirical validation. The model recognized the harsh acceleration of lane changes and helps to explain the reduction of flow. More recently, the authors in (Sala & Soriguera, 2018) provided some empirical findings on freeway lane-changing (B23 access freeway in Barcelona). They confirmed the relation between reduced flow and lane changes: lane changes peaked in congestion periods, and more precisely, downstream of a bottleneck when free flow conditions were recovered. In (Sala & Soriguera, 2020) the authors used the same dataset to quantify the capacity reduction due to the lane-changing activity. However, they did not find empirical evidence that lane changes triggered congestion episodes.

Additionally, in some cities Powered-Two Wheelers (PTWs) have become a popular mean of transport for everyday commuting (E. N. Barmpounakis et al., 2016). However, quantifying their effect on traffic and modeling their driving behavior are complex tasks given their particular characteristics like the unconventional lane-

changing maneuvers or the filtering phenomenon. (Vlahogianni, 2014) studied the kinematic characteristics of PTWs in an urban arterial and their interactions with the other vehicles. Using video recordings, the author also analyzed the factors triggering the filtering phenomenon and the overtakes. In the same direction, (E. N. Barmpounakis et al., 2018) attempted to model the unconventional overtaking patterns of PTWs drivers using meta-optimized decision trees. However, their effect on traffic conditions and how they interact with the rest of vehicle needs to be studied in more detail with the new data that are becoming available to better understand their unique characteristics.

It is seen that studying lane choice and lane changing in urban environments cannot be conducted using the same concepts that are used in motorways. The perturbations in traffic caused by the different modes combined with the drivers' tendency to compete more intensively for the same limited space in order to move faster creates the need for different approaches. While lane changes have been extensively studied for freeways, their relation with stop-and-go effects in congested arterials is unexplored, especially when complex multimodal interactions with heterogeneous drivers are considered. Service-related stops of all relevant modes (taxis, buses, delivery vehicles) create static and moving bottlenecks of different magnitude that are associated with long lane-changing phenomena. With respect to lane choice, empirical evidence is limited as the physical mechanism of the problem requires data that are spatially far and difficult to obtain. Thus, the study of such phenomena using this detailed dataset can allow researchers to better understand the underlying mechanisms of urban congestion propagation and to better model complex phenomena of urban traffic flow.

The current study is conducted in Panepistimiou avenue, a 6-lane arterial which makes it one of the busiest central arterials of Athens. In this paper, we argue that the lanes that are marked on the arterial (marked layer) are influenced by the interactions and frictions created by buses, bus stops, taxi stops, illegal on-street parking, etc. and we show that there is an active layer, which is different to the marked lanes on the road affecting capacity in the macroscopic level and driving behavior in the microscopic. Therefore, two layers are defined regarding how the six lanes of the avenue are actually being used.

# 2. MAIN TEXT

## 2.1 Data processing

### 2.1.1 Description Of The pNEUMA Dataset

The pNEUMA dataset (E. Barmpounakis & Geroliminis, 2020) is the result of a one-of-a-kind field experiment that took place in Athens, Greece in October 2018. A swarm of ten drones flew over the central district of the city recording a massive number of trajectories. The goal of the experiment was to record traffic streams using drones in order to study traffic phenomena in an urban, congested, multimodal and busy environment. Drones provide an excellent point of view from above that allowed to neatly capture all the trajectories. This is, to the authors knowledge, the most exhaustive dataset in such an environment.

Particularly, the swarm of drones covered the central parts of Athens during the morning peak (8:00am-10:30am) each working day of the week. However, the recording process was split into 30-minute sessions due to the limited drone autonomy. Each session included take-off, routing, landing and 15 to 20 minutes of continuous recording. More specifically, there were two take-off/landing locations from where the ten drones would fly to their particular hovering points. Once all the drones would be located in their hovering points, continuous recording of the traffic streams would start.

The result of this experiment is the numerous trajectories that are described with their coordinates in the World Geodetic System (WGS 84) at very high frequency (25 datapoints per second or a datapoint every 0.04 seconds). Features available include position information like speed, acceleration or distance traveled but also vehicle type (car, taxi, PTW, bus, heavy vehicle, and medium vehicle). For more details on the experiment refer to (E. Barmpounakis & Geroliminis, 2020). The data is part of an Open Science initiative and can be downloaded from https://open-traffic.epfl.ch.

### 2.1.2 Area Of Study

Given the fact that the aim of this paper is to study lane changing and lane choice in an urban environment, the area of study should be an arterial with a variety of origin-destination pairs for an adequate sample size. The area chosen is the Panepistimiou avenue, a 6-lane arterial with multiple streets converging and diverging from it. Figure 1 shows the area of study with the traffic streams concerned on top of it (from right to left). The area starts after the turn coming from the most central square of Athens (Syntagma Square) and ends 725m downstream. The street begins as a 6-lane arterial with its leftmost lane as a bus lane in the opposite direction (from x=0m to x=250m). On the other side of the street, the rightmost lane contains several bus stops and unofficial taxi stops. Approximately at x=500m, the rightmost lane ends, and the street becomes a 5-lane arterial. One of the particularities about the avenue is illegal on-street parking in both sides of the road. All these elements create frictions with the traffic streams and will be further analyzed.

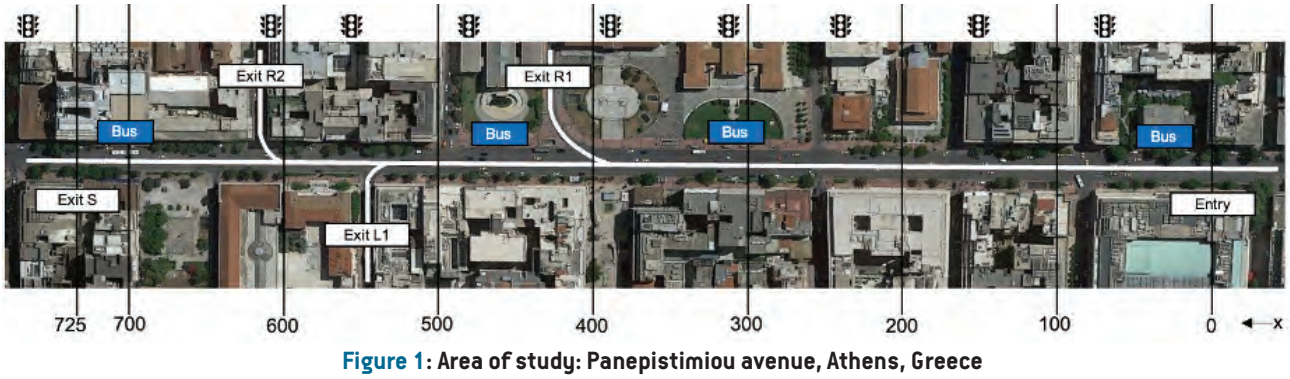


**Figure 1: Area of study: Panepistimiou avenue, Athens, Greece**

The traffic in the street is composed of vehicles coming from upstream as well as vehicles joining from neighboring streets. The vehicles can either continue downstream towards Omonoia Square or turn at one of the multiple streets that stem from Panepistimou avenue. This paper focuses exclusively on the vehicles that join the street at the upstream inlet (x=0m) and continue downstream towards Omonoia Square or turn at one of the three turns in the second half of the area represented in Figure 1: two on the right (x=400m and x=610m) and one on the left (x=530m). Vehicles joining from other intersections are not considered. All these options have been represented with virtual loop detectors that act as virtual checkpoints and allow to classify the vehicles according to their destination. Table 1 summarizes the virtual loops installed in the street to control the destination of each vehicle in the area of study.

The data analyzed spans over 4 different days of the experiment. Specifically, 24/10/2018, 19/10/2018, 30/10/2018, 01/11/2018 and focuses on the last flight session of each day (10:00-10:30 or 10:30-11:00). In total, 1769 vehicles are studied during the four days mentioned above. Of those, the grand majority of the vehicles analyzed (1645) are either cars, taxis, or PTWs; over 90% in all days. More specifically cars and taxis represent more than half of the vehicles (675 cars and 384 taxis) and 586 PTWs add to almost a third. Buses and medium and heavy vehicles are a clear minority in the sample and are therefore removed from the analysis which will then focus on cars, taxis, and PTWs.

With respect to the destination of vehicles the introduction of virtual loops allows to easily keep track of such information. The area is of special interest given that approximately a third of the vehicles turn instead of driving straight towards Omonoia square. Exits R1 and L1 gather over 10% of the vehicles analyzed each. On the other hand, exit R2 has the smallest sample as only 7.52% of the vehicles analyzed turn at the second right turn. Of the 1645 vehicles analyzed, 252 turn at exit R1, 128 turn at exit R2, 168 turn at exit L1, and 1097 continue straight on towards exit S.

**Table 1: Virtual loops to classify vehicles according to their destination**

| Virtual loops | Description | x [m] | Street |
|---|---|---|---|
| Entry | Upstream inlet | 0 | Panepistimiou |
| Exit R1 | First right turn | 400 | Riga Fereou |
| Exit R2 | Second right turn | 610 | Pesmazoglou |
| Exit L1 | First left turn | 530 | Char. Trikoupi |
| Exit S | Downstream outlet | 725 | Panepistimiou |

## 2.2 Defining The Active Layer

One of the main objectives of this paper is to explore vehicle lane choice to better understand how vehicles drive in the urban environment according to their destination. Information at the lane level is therefore essential to conduct such a study. For that purpose, two methodologies were examined regarding how the six lanes were actually being used. On the one hand, the marked layer corresponds to the lanes marked on the road, and their coordinates can be carefully extracted from georeferenced videos. On the other hand, when we apply the lane detection algorithm from (E. Barmpounakis et al., 2020) for an extended arterial an active layer is unveiled, which is different to the marked lanes on the road and affects capacity in the macroscopic level and driving behavior in the microscopic. The main advantage of the active layer is that it shows the real use of the lanes made by drivers. For instance, if a lane is blocked by parked vehicles and vehicles cannot drive on it, this lane is included in the marked layer but since it cannot accommodate any flows it is not included in the active layer. This is illustrated in Figure 2 where an example of blocked lanes is shown; the leftmost lane of the street due to parked vehicles and the rightmost lane due to taxi stops. The active layer therefore provides significant information on the real usage of the available space for drivers that cannot be obtained with the marked lanes on the road.

**Figure 2: Example of blocked lanes**

Since the active layer is the result of running the algorithm along the arterial for every 2 or 5 meters, the lane detection algorithm computes the histogram of vehicles' distances to the edge of the avenue at a specific point and then clusters the histogram with the Jenks natural breaks method. By connecting the breaks -the borders of the lanes- the active lanes are obtained.

The choice of the distance between the clustering points is important because of the different issues that might appear due to the peculiarities of urban traffic. When more conflicts appear in the area, the more in detail must it be analyzed to properly understand and represent the real traffic flows. That is why the use of 2 or 5 meters, depending on the conflict potential, is an adequate choice to guarantee that the active lanes are generally smooth and account for the traffic reality. Additionally, the detection algorithm presents some other parameters to tune, mainly the maximum lane width and the acceptable azimuth difference (direction of movement compared to the north), which are mutually reliant. These ensure that the result provided by the algorithm is realistic. After a trial-and-error process, the parameters chosen to run the detection algorithm were 10 degrees as the maximum acceptable azimuth difference and 4m as the maximum lane width.

In order to build the active layer several possibilities were considered: clustering the trajectories of one of the days available in the dataset or using all the data combined. All the possibilities were then tested, and it was decided that only the trajectories of Thursday 1/11/18 would be considered to build the active lanes. It should be noted that PTWs were excluded in all cases as they would act as noisy data to the calculation of the active layer. Although the data from the other days provided similar outputs and indicated very similar frictions, the trajectories of Thursday 1/11/18 provided the highest recognized area as well as the smoothest lane borders. Furthermore, there were no elements on that specific day to twist the traffic information.

### 2.2.1 Marked vs. Active Layer Analysis

Figure 3 shows the differences between both layers. The crosses indicate those parts of the marked lanes that have not been included in the active layer. Of the six lanes of the avenue, only lanes 2, 3 and 4 are continuous. On the left side of the street, lane 1 is detected only in the final part of the arterial. As previously mentioned, lane 1 is actually a bus lane in the opposite direction in the beginning of the street and then becomes blocked due to illegal on-street parking. The lane is only first recognized before the left turn (Exit L1) due to the traffic stream coming from lane 2 to turn left. After the left turn vehicles recover progressively the lane and it is again detected. In the right part of the street there are more elements that can create frictions: high presence of buses, bus stops, unofficial taxi stops, parked vehicles, etc. These elements are the main reason why the rightmost lane is partially blocked. At the beginning of the avenue, lane 6 is blocked due to parked vehicles and a taxi stop just upstream. Buses drive mainly on lane 5 and recover lane 6 when they approach the Akademia bus stop, which is one of the most important transportation hubs in the avenue. After the Akademia bus stop, unofficial taxi stops occupy lane 6 preventing other vehicles from using it. Regarding lane 5, it starts as a continuous lane but becomes blocked when lane 6 ends. Then, it becomes the rightmost lane and suffers from the same issues: bus stops and parked vehicles. That is why after a certain point lane 5 becomes blocked and vehicles merge into lane 4. Consequently, the street becomes a 3-lane arterial in reality (only lanes 2, 3 and 4 are available). This situation lasts until lane 1 is recovered shortly after the left turn. With regards to the right turns, there are no separated turning lanes detected as opposed to the left turn in exit L1.

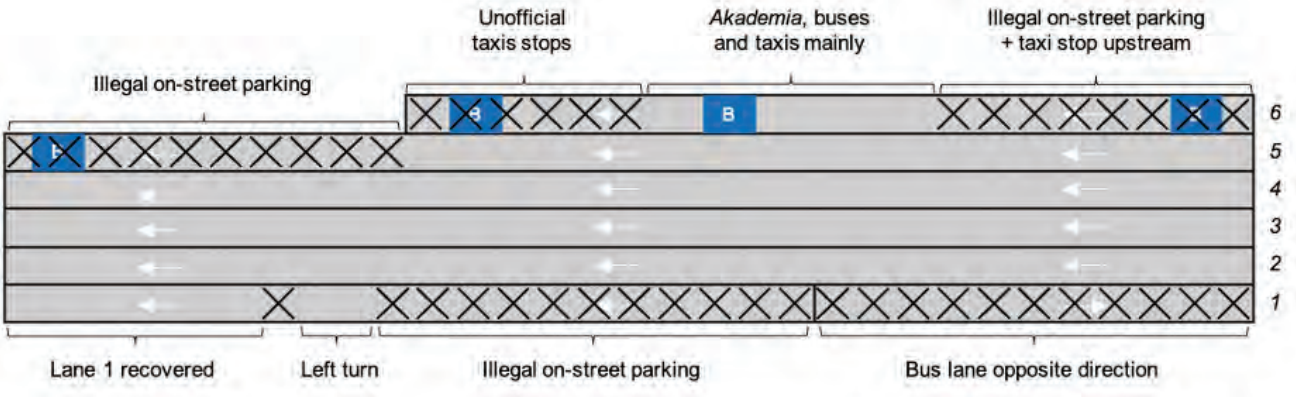


**Figure 3: Outline of the active layer**

### 2.2.2 Lane assignment

The study of traffic at the lane level requires to assign a lane to each vehicle along its trajectory. Each datapoint was therefore assigned to a lane so that we could keep track of the lane changes and the lane choice of vehicles. For that purpose, by the results of the lane detection points every 2 or 5 meters, the associated clustering points were connected and converted into polygons that formed the lanes. This resulted in an easy lane assignment process: it sufficed to check which polygon contained each datapoint for each vehicle. It should be noted that for the characteristic points at the edges of the active layer, all points of the road between them and the edges of the marked layer were assigned to the nearest detected lane to the border.

Once all the points of the trajectories were allocated to a lane, a smoothing process of the lane assigned was performed to guarantee the veracity and continuity of the lane assigned. Indeed, not applying any kind of smoothing would have resulted in an unrealistic number of lane changes caused by the high

frequency of the data and the irregularity of lane borders. After a sensitivity analysis, it was concluded that a rolling average with a 5-observation moving window was adequate to provide the most accurate results.

## 2.3. Lane Changing

In this section, the data at the lane level was utilized to study lane changing. The identification of lane changes consists in checking the points where the trajectory changes the lane that has been assigned. Compared to the methodology described in (E. Barmpounakis et al., 2020) , this method can provide more accurate results, mostly because it is less sensitive to maneuvers that did not result in an actual lane change.

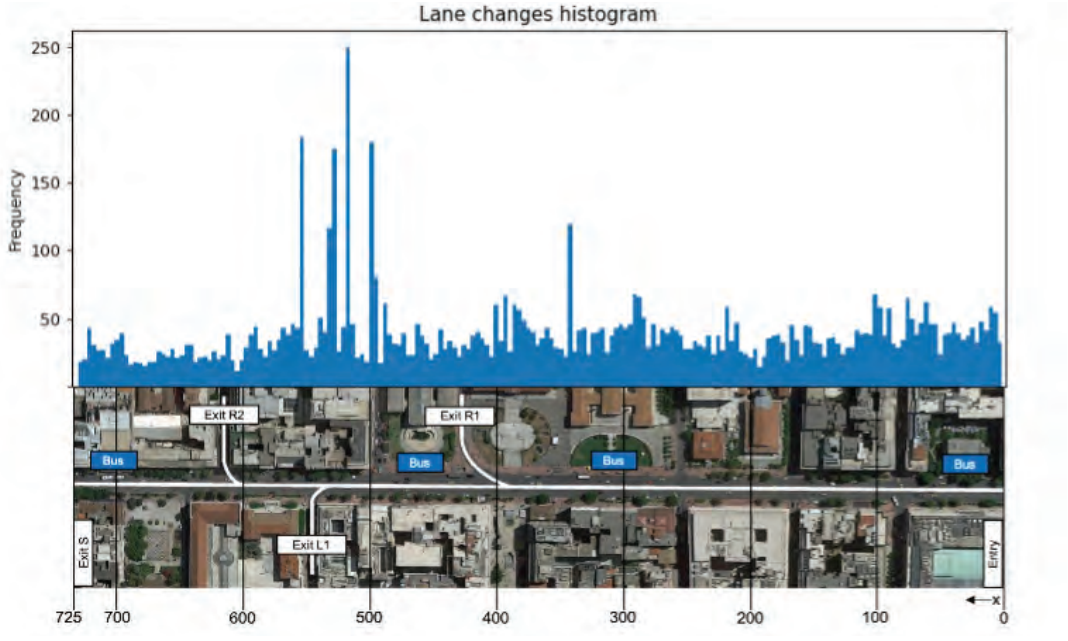


**Figure 4: Histogram of lane changes locations**

Figure 4 shows a histogram of the locations where lane changes take place. The data shows that there is a more or less constant lane-changing rate and some very well-defined peaks. The activity decreases in the last 100 meters of the street as an important proportion of vehicles have left the street. The fact that the active layer represents the real use of the street allows to easily spot those areas in the street that are susceptible to high lane-changing activity. These areas coincide with the points where lanes are firstly recognized or blocked: the peak at x = 340m corresponds to the block of lane 6 in the right part of the street and the peak at x = 500m represents the block of lane 5. The peaks at x = 500m, x = 510m and x = 530m coincide with the detection of lane 1. It is seen that those peaks represent the potential merging points and thus the methodology can identify points of the network where capacity of an arterial is reduced/increased, even for a short length.

The trajectories analyzed not only allow to study the parts of the street where lane changes are more frequent but also the relation between lane changes and other variables, i.e., the vehicle type or the destination. This is precisely the information provided by the boxplots in

Figure 5. The boxplots shown in this section are composed of the interquartile range (main blue box), the median (black line), the mean (green triangle), the 1% and 99% whiskers and the outliers.

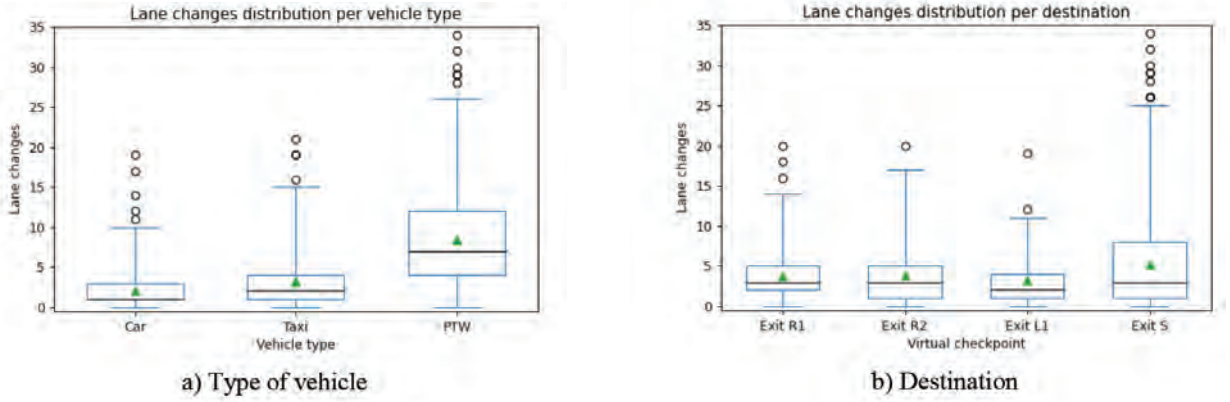


**Figure 5: Distributions of the number of lane changes performed per a) type of vehicle and b) destination**

Figure 5a shows the lane-changing distribution for each type of vehicle. The majority of cars and taxis, at least 75%, performed less than 5 lane changes. However, there is a tendency for cars to perform less lane changes: the mean for cars is 2.08 whereas taxis performed 3.20 changes on average. The taxi distribution has also a higher standard deviation, meaning that there is more diversity in the taxi behavior. The fact that taxis drive on the right part of the street, where friction elements prevent from having continuous lanes, as well as occasional stops might be responsible for such results. Welch t-tests (t-test assuming different variances and sample size) confirm that there are significant differences among the distributions: p-value tends to zero in all cases.

Figure 5a also allows to confirm that PTWs have a completely different behavior. Indeed, the number of lane changes is much higher than for the other types of vehicles; average of 8.44 lane changes. Half of the PTWs analyzed did a maximum of 7 lane changes and only 25% performed 4 or less changes. This heavily contrasts with the car and taxi distributions. Additionally, there are 25% of the sample observations that performed more than 12 changes. This behavior is a clear hint of the PTWs' filtering phenomenon; overtake other larger vehicles by driving on the edge of the lanes creating a faster stream between them. More specifically, a big proportion of the lane changes detected are a consequence of small lateral movements in the edges of the lanes. A more detailed description of this traffic phenomenon follows in the next subsection.

With regards to the lane changes per destination,

Figure 5b presents the boxplots for all types of vehicles in each destination. Intuitively, the vehicles driving towards exit S performed more lane changes as their trajectories are longer; they performed 5.11 changes on average, which corresponds to the highest average value. Moreover, there are 25% of the observations in the exit S distribution that performed 8 or more lane changes. These observations are in their majority classified as PTWs. On the other hand, turning vehicles performed less lane changes since their trajectories are shorter. Vehicles turning right have a very similar distribution and vehicles turning left have the lowest distribution in terms of changes. The Welch t-test confirms that the average number of lane changes of right-turning vehicles (3.71 for exit R1 and 3.84 for exit R2) cannot be considered statistically different. Left-turning vehicles performed less changes (3.23 on average) and have the smallest standard deviation. This is the consequence of similar trajectories due to the absence of frictions on the left part of the street and will be further analyzed in the lane choice section.

### 2.3.1 PTW Filtering

As discussed before, the lane-changing distribution for PTWs gave a hint of a completely different behavior. In this section, additional evidence of such behavior is provided. In order to have more meaningful results, only vehicles going straight will be analyzed since they represent the largest sample and perform more lane changes.

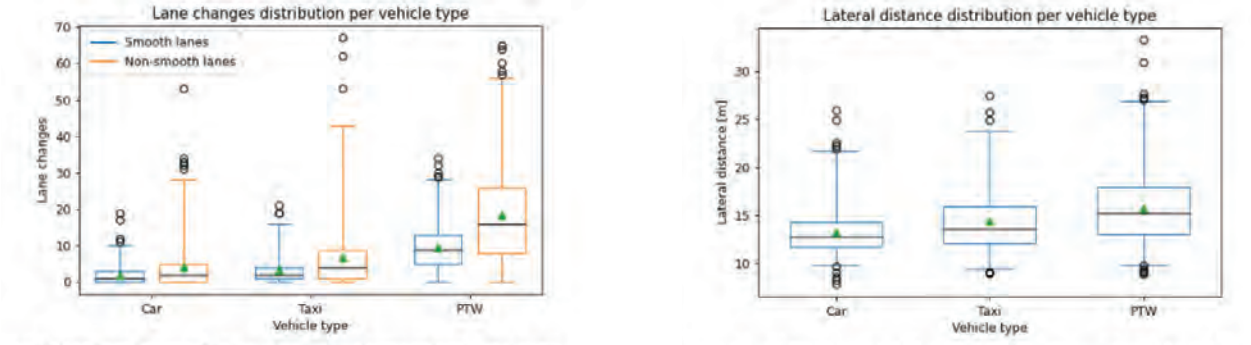


a) Distributions of lane changes (smoothed and non-smoothed lanes) for straight vehicles

b) Distributions of the lateral distance traveled for straight vehicles

**Figure 6: Lane changes and lateral distance distributions for each type of vehicle**

The lane assignment process described in the methodology includes a smoothing of the lane allocated. This is done to avoid non-realistic lane changes caused by the high frequency of the data and the noisy edges of the active lanes. Yet,

Figure 6a presents the lane changes for straight vehicles when the lane assigned has been smoothed and when it has not. The orange boxplots (no smoothing) show a novel visualization of the filtering phenomenon. When the lane assignment is not smoothed the differences between the types of vehicles are accentuated. On average, PTWs perform 18.34 changes whereas cars and taxis perform 4.13 and 6.74, respectively. Furthermore, the PTWs' distribution is clearly above the cars' and taxis'. The lane assignment, thus, captures the relative position of PTWs inside the lanes. They do not drive in the middle of the lanes like cars and taxis. Instead, the drive between the vehicles in the edges of the lanes. Since these edges are noisy from the detection algorithm, more lane changes are detected in this area providing evidence of the filtering phenomenon.

Another relevant aspect to the filtering phenomenon is the lateral distance traveled along the street. The lateral distance

is a consequence of the lane changes and small deviations inside the lane. Intuitively, every time a vehicle performs a lane change its lateral distance traveled should increase by approximately the width of the lanes. However, this is not always the case since vehicles perform different types of lane changes and do not always drive on the center of the lane.

Figure 6b shows the lateral distance traveled distribution for cars, taxis, and PTWs. PTWs drive more lateral distance than taxis and cars, and taxis drive more lateral distance than cars. Moreover, a Welch t-test shows that all the distributions are statistically different. The results are very relevant and interesting due to the difference in the nature of the lane changes performed by PTWs and the other vehicles. PTWs tend to perform a lot of small narrow lane changes in the edges of lanes while cars and taxis perform wide lane changes to move towards another lane. In a typical car change, the lateral distance traveled is approximately the width of the lanes and is much higher than in a typical PTW narrow change. This provides more evidence on the filtering phenomenon; while cars and taxis perform wider and less lane changes, PTWs perform narrower and more lane changes that result in a higher lateral distance traveled.

## 2.4 Lane choice

As it was discussed in the literature review section, drivers choose the lane they drive on considering their destination, traffic conditions, surrounding vehicles and many other factors. In this context, vehicles perform different types of lane changes: discretionary changes to overtake slower or bigger vehicles, preemptive changes to anticipate a turn downstream and move towards the turning lane and mandatory changes if needed.

In this section special interest is given to turning vehicles. Thus, the analysis of the lane choice below is done according to their destination. The first analysis concerns the way turning vehicles approach the target -or turning- lane, meaning the lane used just before they turn.

The target lane for vehicles turning at the first right turn (exit R1) is lane 5, as lane 6 is occupied due to the Akademia bus stop and an unofficial taxi stop. In the case of the second right turn (exit R2) the target lane is lane 4, being lane 5 blocked by illegal on-street parking. Finally, the target lane for vehicles turning left in exit L1 is lane 2, as lane 1 is also blocked due to illegal on-street parking.

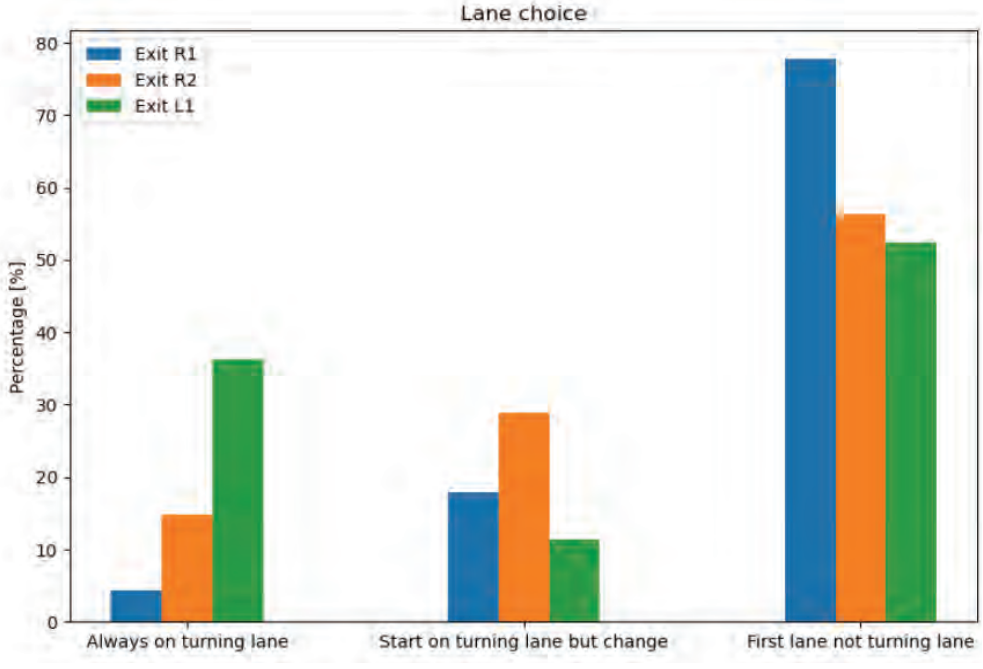


**Figure 7: Initial lane choice**

Figure 7 presents a first representation of the choice made by turning vehicles. Vehicles were split into i) those that always drive on the target lane, ii) those that start on the target lane but eventually perform at least one lane change and return to the target lane, and iii) those who do not start driving on the target lane and are therefore forced to change the lane. Only a small percentage of the right-turning vehicles drove always on the target lane (4.37% and 14.84% for exits R1 and R2, respectively). On the other hand, over 36% of the left-turning vehicles stayed always on the target lane. This difference is a consequence of the stability of the left part of the street: there are no interactions with buses and taxis and there are less frictions. In addition, lane 1 was always blocked meaning that left-turning vehicles had a clear target lane (lane 2). The second group of vehicles refers to those that performed at least one discretionary change -they started driving on the correct lane but eventually changed it. This characteristic is especially noted for vehicles turning at exit R2. A possible explanation concerns the perception of lane 4 as a central lane at the beginning of the street and the fact that the turn is located much downstream. Contrary, the majority of vehicles turning left that started on the target lane continued until the turn and a small percentage did

eventually perform a discretionary change. However, the most important group for the three turning exits comprises the vehicles that did not start driving on the target lane. These vehicles performed both discretionary and preemptive lane changes. Regarding the first right turn, even if it is the closest turn to the beginning of the street, most of the vehicles did not start on lane 5. Instead, most chose lanes 4 and 3. This is due to the high presence of buses on lane 5, being lane 6 blocked at the beginning of the avenue. Finally, straight vehicles need another type of analysis: they perform only discretionary and mandatory changes. 86% of the straight vehicles performed at least 1 change and only 14% never changed the lane.

Another powerful and visual way to illustrate the choice of lane consists in building successive histograms along the avenue for each destination. For that reason, the avenue was split into 5-meter segments, and for each particular segment the lane each vehicle was most of the time was checked. The successive histograms are represented with heatmaps in Figure 8.The crosses indicate those parts of the lanes blocked.

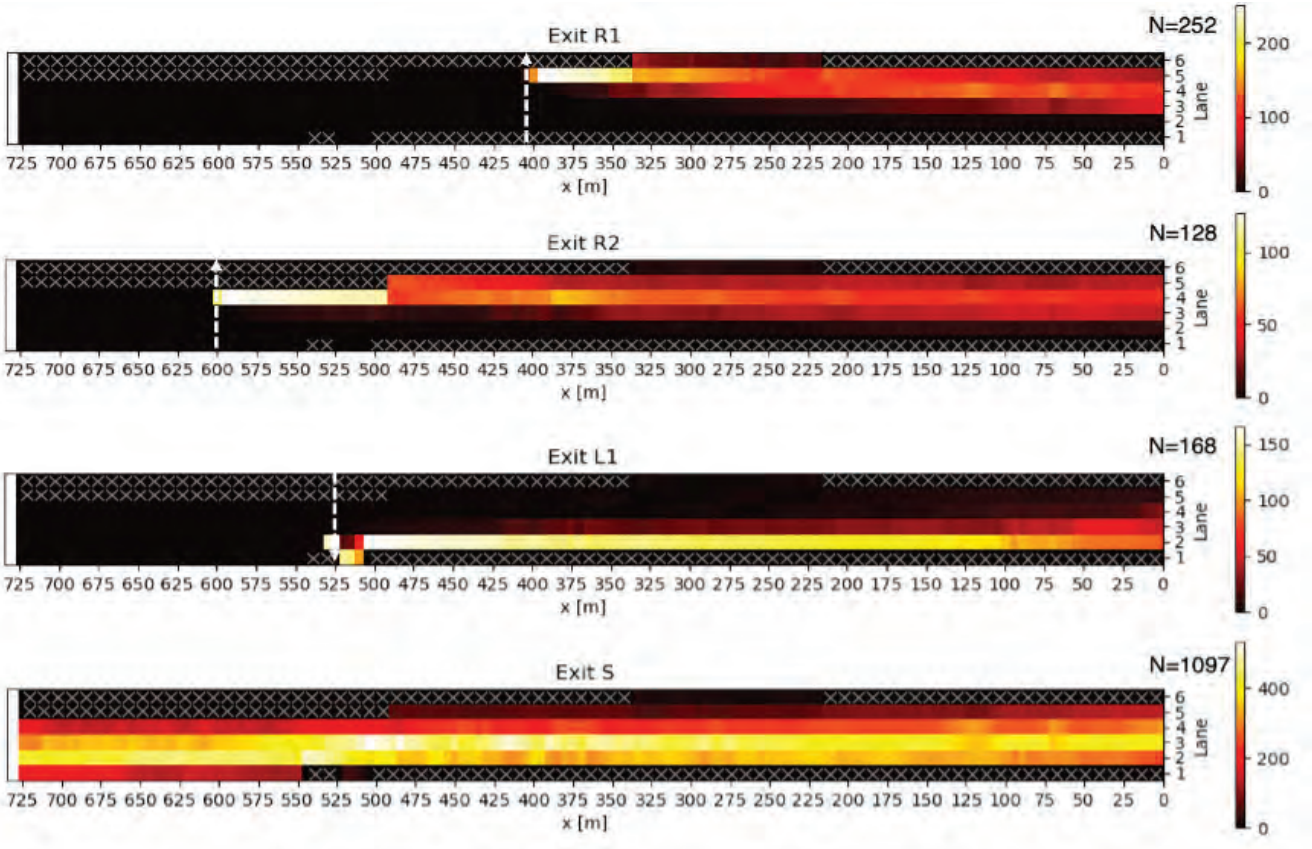


**Figure 8: Histograms of the lane chosen every 5 meters**

The first heatmap referring to exit R1 shows that although vehicles mainly started in lanes 3 and 4, they congregated in lanes 4 and 5. Indeed, vehicles tent to abandon lane number 3 to join lane 4. Lanes 4 and 5, thus, gathered most of the traffic until the last 125 meters before the turn. It was then that the majority of vehicles coming from lane 6 on the right and lane 4 on the left moved towards the turning lane. Therefore, there was a big proportion of the vehicles that waited until the last 100 meters approximately to move towards the target lane. This choice is logical from the perspective of the frictions in the right part of the street, and more especially by the presence of buses on lane 5 and the bus stop Akademia just before, as it was also seen in Figure 4. In the case of vehicles turning right at exit R2, they suffered from similar frictions as the ones turning right before. Yet, since the turn is located further downstream the first 300 meters do not show any evolution. Here, the choice was heavily influenced by the bottleneck caused by the block of lane 5. Some vehicles chose lane 5 after vehicles turning at exit R1 left the avenue but were eventually forced to merge into lane 4. From the left side, vehicles stayed on lane 3 much longer but joined progressively the target lane. The heatmap clearly shows that in the last 100 meters vehicles used exclusively lane 4. With regards to the left turn, a completely different choice model can be identified. Even if over 50% of the vehicles did not choose the target lane at the beginning of the avenue (Figure 7), they concentrated in lanes 2 and 3 rapidly. Additionally, vehicles left lane 3 progressively to join the target lane, but most of them anticipated the change very early unlike the right-turning vehicles analyzed. The absence of frictions in the left part of the road provides a stability that translates into a smooth transition towards the target lane. Moreover, the very last part of the turning trajectories shows how all the vehicles took the recognized segment of lane 1. After using lane 1 vehicles left the avenue and did not use lane

2 as suggested in Figure 8, which stems only from the construction of the active layer. Finally, the choice of straight vehicles reflects that vehicles preferred to use lanes 2, 3, and 4 for they were the only continuous lanes along the avenue. Lane 5 was quickly abandoned as it was mainly used for buses and turning vehicles and is close to the friction elements in the right border. Lane 3 was the most popular lane at the beginning of the street as it avoided both left- and right-turning vehicles. However, after the left turn (exit L1), lane 1 was open to the traffic and the available part of the street was shifted to the left. Lane 2 became the most popular lane as it was emptied from the turning vehicles.

### 2.4.1 Last Lane Change To Join The Target Lane

Another interesting aspect about lane choice concerning turning vehicles is the last lane change made to join the target lane before the turn. Figure 9 presents a series of metrics regarding that particular last lane change. An important concept here is the distance to turn, meaning the distance between the last lane change and the turning point (point where the lane assignment is no longer viable). Metrics include the distribution of the distance to turn, distribution of speed and the relations of the distance to turn with lateral acceleration and speed.

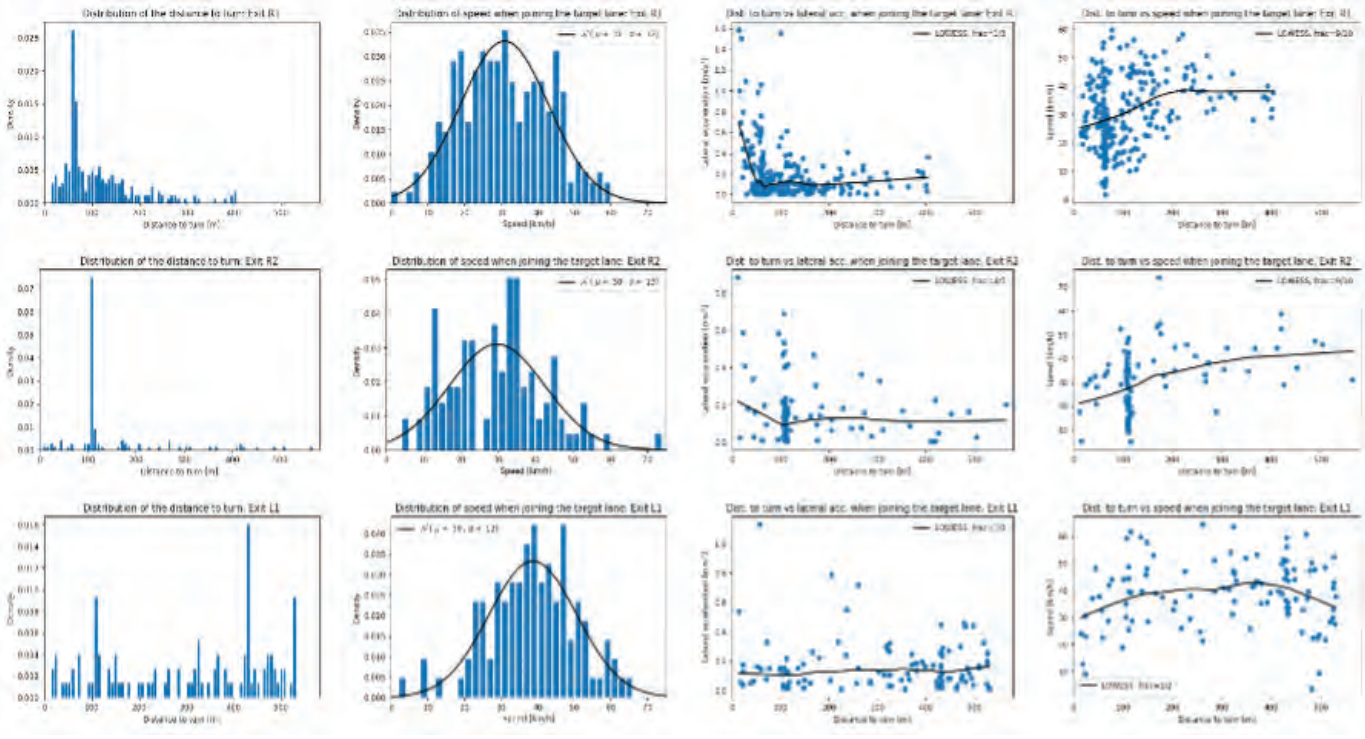

**Figure 9: Metrics of the last lane change to join the target lane**

The distributions of the distance to turn in Figure 9 again show that a majority of right-turning vehicles joined the target lane in the last 100 meters. More in detail, the case of exit R2 shows a well-defined peak around 100m corresponding to the block of lane 5 where vehicles were forced to merge into lane 4. Regarding left-turning vehicles, the histogram shows that there was no specific location in which the majority of the vehicles joined the turning lane. Instead, there was a smooth transition towards the turning lane and vehicles gradually joined the turning lane at their convenience.

This gradual process results in a speed distribution shifted to the right -faster- compared to the right turns. The histograms resemble approximately normal distributions centered around 30 km/h and 40km/h for right- and left-turning vehicles, respectively. There is thus, a difference in behavior: right-turning vehicles waited until the last 100 meters approximately to join the turning lane avoiding the interactions with buses and other frictions and left-turning vehicles could anticipate the turn by moving towards the target lane at their convenience.

Additional evidence of such difference in behavior is given by the relations between the distance to turn and the lateral acceleration and speed. The scatter plots for right-turning vehicles show that vehicles that waited until the last moment to turn have a higher lateral acceleration in absolute value. This can be interpreted as a sign of driver aggressiveness as drivers were forced to quickly join the turning lane before it was too late. Nonetheless, the relation in the case of exit R2 is not as evident due to smaller sample size and the fact that there is a point that concentrated the majority of the observations. As for left-turning vehicles, the trend is non-existent because most of the drivers anticipated the turn and were not forced to perform a sudden move to turn. Additionally, by comparing the distance to turn and the speed in the last lane change we discover that those vehicles performing the last change with a

lot of anticipation could afford to drive faster. On the contrary, drivers that waited until the last moment had to be forced to reduce their speed: the scatter plots shows that low speeds are related to small distances to turn.

### 2.4.2 Lane Speed

An interesting aspect about lane choice is the role of speed. It is believed to play a key role on discretionary lane changes since they are associated with vehicles willing to overtake to improve their traffic conditions. However, speed is highly correlated with the particular context of each part of the street. Figure 10 shows the average speed of cars and taxis -PTWs not included- driving in each lane for segments of 10 meters along the street. Only observations with speed higher than 15km/h were considered to avoid stopped vehicles due to traffic lights or service-related stops.

The speed profiles of Figure 10 suggest that there are important differences between lanes on the left and lanes on the right part of the road. Indeed, vehicles driving on the left lanes have a higher speed than those driving on the rightmost lanes. This difference in speed is influenced by the friction elements already mentioned in the right border of the street. The presence of the buses driving on them is a key factor. Even if the number of buses on the dataset is small compared to cars and taxis, their sole presence on the street implies a speed reduction in the rightmost lanes where buses tend to drive on. Another general remark is that the speed of a lane used by turning vehicles is rapidly recovered right after they leave the street.

While the general trend described above is valid for the whole length of the street, the speed profiles in each lane evolve as a function of the context. Before exit L1, lane 1 acts as a small turning lane and vehicles are forced to reduce the speed in order to turn. Once the lane is recovered after the turn, the speed becomes very high since few vehicles use it. On the other hand, lanes 2 and 3 have a similar behavior. Like all the lanes their speed starts in a short plateau and rises to more than 40 km/h. Compared to the other lanes, they do not suffer a speed drop around x=180m. Still, their speed is gradually reduced until the street becomes a 3-lane arterial when the vehicles drive at their lowest speed. Once the street becomes a 4-lane arterial again the speed is recovered and lane 2 becomes even faster than lane 3. Finally, lanes 4 and 5 also have a close behavior. Vehicles increase their speed until x=180m more or less and after this point their speed starts to drop. This speed reduction is probably due to the short interaction of vehicles with lane 6 and the approaching bus stop at x=300m. After the bust stop, lane 5 ends at x=500m due to illegal on-street parking and vehicles are forced to join lane 4. This results in a speed reduction that affects all the lanes since the street becomes a 3-lane arterial for a short length.

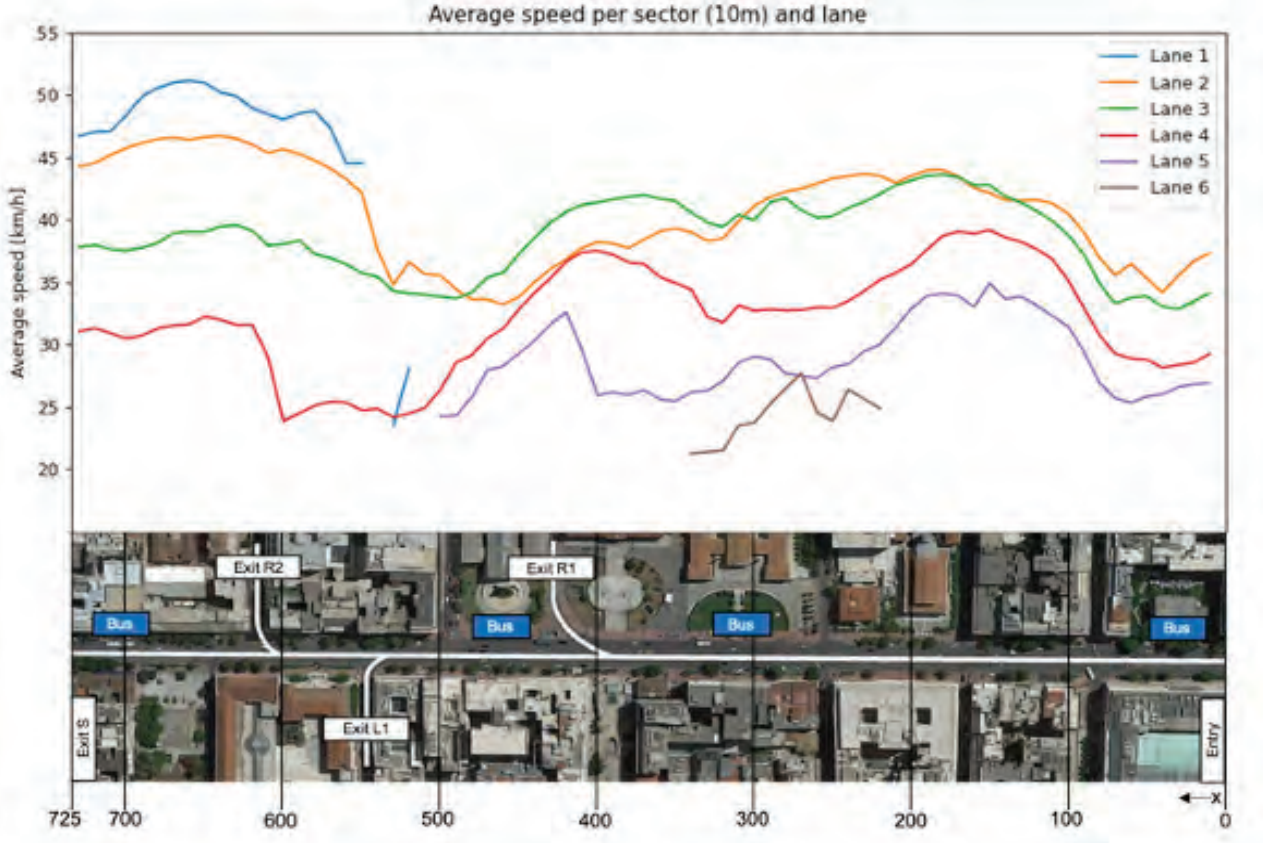


**Figure 10: Average speed profile per lane**

## 3. CONCLUSIONS

The pNEUMA dataset offers a unique opportunity to study traffic phenomena in a multimodal and urban environment. This research shows the potential of how detailed datasets together with powerful analysis tools can be useful to model how vehicles drive in cities and help us to better understand possible causes of congestion's formation and propagation. Firstly, the use of a lane detection algorithm allows to extract the traffic information at the lane level and to recognize the active usage of the available space to traffic made by drivers. We show that the existence of an active layer unveils that illegal on-street parking as well as frictions in the right part of the street like buses, bus stops, or unofficial taxi stops reduce the capacity of the avenue. It was seen that in some areas of the 6-lane avenue, the lanes that can actually accommodate traffic are reduced to only 3.

The analysis conducted in lane-changing activity shows a constant lane-changing rate. Using this methodology, when a sudden high level of lane changes is detected, it implies conflicting areas like lane blocks. Additionally, the analysis of lane changes with regards to the types of vehicles shows the different way vehicles are conducting lane changing maneuvers. PTWs perform more lane changes than taxis, which then perform more changes than cars. In the case of taxis, as they perform occasional stops and drive mainly on the right part of the street due to their service-related stops or when looking for passengers, interactions with buses and other frictions of the right side of the road can be detected. Regarding PTWs, evidence on the filtering phenomenon is provided as they perform more lane changes as a consequence of small lateral deviations in the borders between lanes. Their distinct driving behavior is further presented as these lateral deviations result in a higher average lateral distance traveled with respect to cars and taxis.

Then, vehicles are split according to their destination to account for the differences between left-turning, right-turning, and straight vehicles. The study on lane choice highlights the difference in behavior for left- and right-turning vehicles as well as the importance of preemptive changes in an urban context. Left-turning vehicles do not interact with the friction elements on the right part of the street and can afford to anticipate the turn much before than right-turning vehicles. The left-turning vehicles analyzed performed a smooth transition towards the turning lane. Furthermore, a big proportion of the vehicles analyzed never performed a lane change and they drove always on the target lane to turn.

Those that joined the turning lane along did it at their convenience and at their desired speed -speed distribution at the last lane change is higher than for vehicles turning right-. In contrast, right-turning vehicles present a variety of situations heavily influenced by the context of the street. Indeed, the last change before the turn is heavily triggered by the presence of buses and the lane blocks in the rightmost lanes. Distributions show that vehicles waiting to join a right-turning lane in the last moment had higher lateral acceleration and were forced to reduce their speed. With regards to straight vehicles, they tended to drive in the central and left lanes trying to avoid the frictions of the right lanes. The lane changes they perform are exclusively to overtake other vehicles and improve their driving conditions. Only 14% of the straight sample never changed a lane.

The findings that are presented in this study provide a significant contribution regarding the lane choice process of drivers in an urban environment. Future research attempts will aim to use the results on lane changing and lane choice to develop models that predict the driver's intention to turn. This will allow to better understand and differentiate turning and straight vehicles.


### ACKNOWLEDGEMENTS

*The authors would like to acknowledge the partial funding supported by the EPFL Open Science Fund and Swiss National Foundation project 200021_188590.*

**4. References - Bibliography**


- Barmpounakis, E., & Geroliminis, N. (2020). On the new era of urban traffic monitoring with massive drone data: The pNEUMA large-scale field experiment. *Transportation Research Part C: Emerging Technologies, 111*(October 2019), 50–71. https://doi.org/10.1016/j.trc.2019.11.023
- Barmpounakis, E. N., Vlahogianni, E. I., & Golias, J. C. (2016). Intelligent Transportation Systems and Powered Two Wheelers Traffic. IEEE *Transactions on Intelligent Transportation Systems*, *17*(4), 908–916. https://doi.org/10.1109/TITS.2015.2497406
- Barmpounakis, E. N., Vlahogianni, E. I., & Golias, J. C. (2018). Identifying predictable patterns in the unconventional overtaking decisions of PTW for Cooperative ITS. IEEE *Transactions on Intelligent Vehicles, 3*(1), 102–111. https://doi.org/10.1109/TIV.2017.2788195
- Barmpounakis, E., Sauvin, G. M., & Geroliminis, N. (2020). Lane Detection and Lane-Changing Identification with High-Resolution Data from a Swarm of Drones. *Transportation Research Record, 2674*(7), 1–15. *https://doi.org/10.1177/0361198120920627*
- Choudhury, C. F., & Ben-Akiva, M. E. (2008). Lane Selection Model for Urban Intersections. *Transportation Research Record: Journal of the Transportation Research Board*, *2088*(1), 167–176. https://doi.org/10.3141/2088-18
- Gipps, P. P. G. (1986). A model for the structure of lane-changing decisions. *Transportation Research Part B: Methodological*, *20*(5), 403–414. https://doi.org/10.1016/0191-2615(86)90012-3
- Kesting, A., Treiber, M., & Helbing, D. (2007). General Lane-Changing Model MOBIL for Car-Following Models. *Transportation Research Record: Journal of the Transportation Research Board, 1999*, 86–94. https://doi.org/10.3141/1999-10
- Laval, J. a., & Daganzo, C. F. (2006). Lane-changing in traffic streams. *Transportation Research Part B: Methodological, 40*(3), 251–264. https://doi.org/10.1016/j.trb.2005.04.003
- Lu, W., Rui, Y., & Ran, B. (2020). Lane-Level Traffic Speed Forecasting: A Novel Mixed Deep Learning Model. *IEEE Transactions on Intelligent Transportation Systems*. https://doi.org/10.1109/TITS.2020.3038457
- Sala, M., & Soriguera, F. (2020). Lane-changing and freeway capacity: A Bayesian inference stochastic model. C*omputer-Aided Civil and Infrastructure Engineering, 35*(7), 719–733. https://doi.org/10.1111/mice.12529
- Sala, M., & Soriguera, F. (2018). Freeway lane-changing: Some empirical findings. *Transportation Research Procedia, 33*, 107–114. https://doi.org/10.1016/j.trpro.2018.10.082
- Sun, D. J., & Elefteriadou, L. (2012). Lane-Changing Behavior on Urban Streets: An "In-Vehicle" Field Experiment-Based Study. *Computer-Aided Civil and Infrastructure Engineering, 27*(7), 525–542. https://doi.org/10.1111/j.1467-8667.2011.00747.x
- Toledo, T., Choudhury, C. F., & Ben-Akiva, M. E. (2005). Lane-Changing Model with Explicit Target Lane Choice. *Transportation Research Record: Journal of the Transportation Research Board, 1934*(1), 157–165. https://doi.org/10.1177/0361198105193400117
- Toledo, T., Koutsopoulos, H. N., & Ben-Akiva, M. E. (2003). Modeling Integrated Lane-Changing Behavior. T*ransportation Research Record, 1857*, 30–38. https://doi.org/10.3141/1857-04
- Vlahogianni, E. I. (2014). Powered-Two-Wheelers kinematic characteristics and interactions during filtering and overtaking in urban arterials. *Transportation Research Part F: Traffic Psychology and Behaviour, 24*, 133–145. https://doi.org/10.1016/j.trf.2014.04.004
- Wei, H., Lee, J., Li, Q., & Li, C. J. (2000). Observation-Based Lane-Vehicle Assignment Hierarchy: Microscopic Simulation on Urban Street Network. *Transportation Research Record: Journal of the Transportation Research Board, 1710*(1), 96–103. https://doi.org/10.3141/1710-11



***Jasso Espadaler Clapes*[1]*, Emmanouil Barmpounakis*[1]*,***
***Nikolas Geroliminis*[1]**
[1]Ecole Polytechnique fıdırale de Lausanne - EPFL


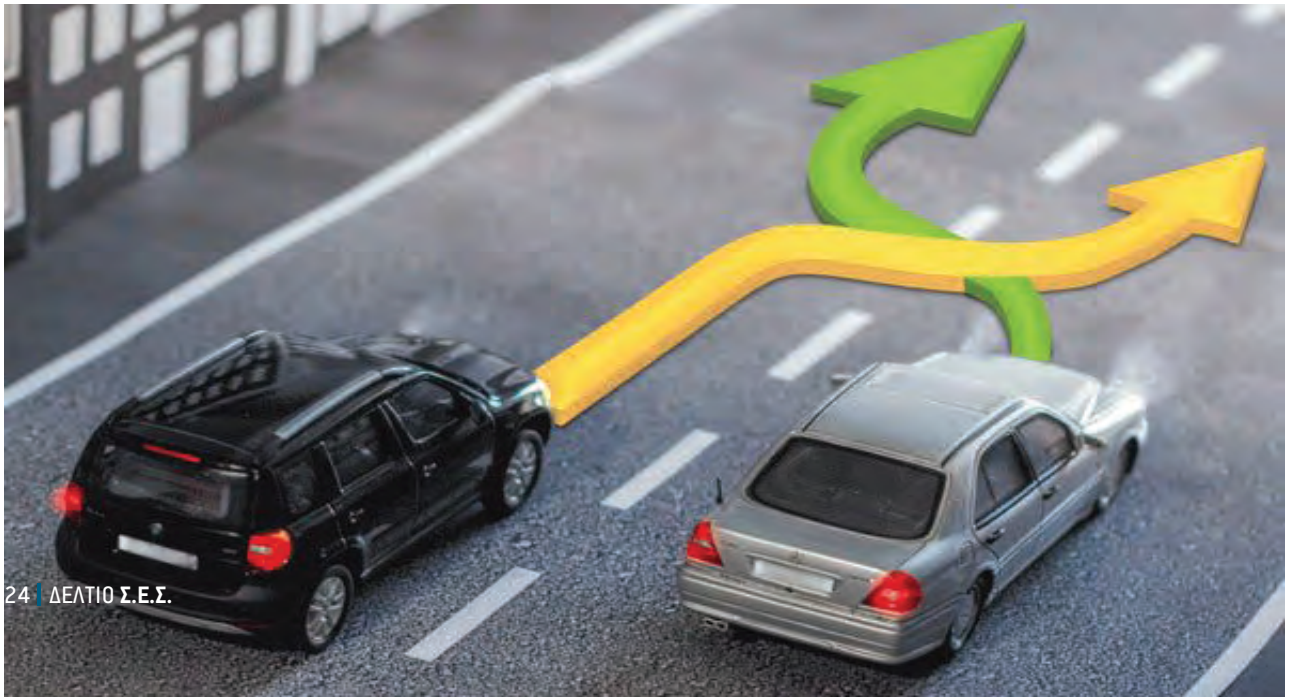

Για τη συγγραφή του παρόντος άρθρου, απονεμήθηκε στη Νέα ερευνήτρια **Εύα Μιχελαράκη** το Βραβείο για την Καλύτερη Επιστημονική Εργασία στην Οδική Ασφάλεια κατά τη διάρκεια του 10ου Διεθνούς Συνεδρίου για την Έρευνα στις Μεταφορές (ICTR 2021)

# Modelling the Safety Tolerance Zone: Recommendations from the i-DREAMS project

**Eva Michelaraki[1*], Christos Katrakazas[2], Tom Brijs[3], George Yannis[4]**

## ABSTRACT

The i-DREAMS project aims at defining, developing, testing and validating a "Safety Tolerance Zone" (STZ) in order to prevent drivers from getting too close to the boundaries of unsafe operation by mitigating risk in both real-time and post-trip. The aim of the current study is to provide guidelines for mapping the concept of the STZ using continuous variables of risk and the most reliable indicators (e.g. time headway, speed, harsh acceleration, distraction) are going to be investigated in real-time. For the purpose of the analysis, a variety of analytical methods and potential modelling approaches are proposed. According to the research question made, a mapping exercise of machine learning algorithms (e.g. Long Short-Term Memory or Dynamic Bayesian Networks) is implemented for real-time data prediction. The key output will be the correlation of the aforementioned explanatory variables and various indicators of task complexity and coping capacity with the dependent variable risk.

***Keywords:*** *i-DREAMS project, safety tolerance zone, mapping methodology, continuous risk indicators, real-time prediction.*

## ΠΕΡΙΛΗΨΗ

Το έργο i-DREAMS στοχεύει στον ορισμό, την ανάπτυξη, τη δοκιμή και την επικύρωση του "εύρους ανοχής ασφαλείας" (STZ), ώστε να αποφευχθεί η υπερβολική απόκλιση των οδηγών από τα όρια της ασφαλούς λειτουργίας, μειώνοντας τον κίνδυνο τόσο σε πραγματικό χρόνο όσο και μετά το ταξίδι . Στόχος της παρούσας μελέτης είναι να παρέχει οδηγίες για τη χαρτογράφηση της έννοιας της STZ χρησιμοποιώντας συνεχείς μεταβλητές κινδύνου και οι πιο αξιόπιστοι δείκτες (π.χ. απόσταση προπορευόμενου οχήματος, ταχύτητα, απότομη επιτάχυνση, απόσπαση προσοχής) θα διερευνηθούν σε πραγματικό χρόνο. Για τον σκοπό αυτό, προτείνονται αρκετές μέθοδοι ανάλυσης και προσεγγίσεις μοντελοποίησης. Σύμφωνα με τις ερευνητικές ερωτήσεις που πραγματοποιήθηκαν, διάφοροι αλγόριθμοι μηχανικής μάθησης (π.χ. Long Short-Term Memory ή Dynamic Bayesian Networks)

εφαρμόζονται για την πρόβλεψη δεδομένων σε πραγματικό χρόνο. Το βασικό αποτέλεσμα θα είναι η συσχέτιση των προαναφερόμενων επεξηγηματικών μεταβλητών και των δεικτών πολυπλοκότητας που σχετίζονται με την οδήγηση με τον εξαρτώμενο κίνδυνο.

***Λέξεις - κλειδιά:*** *Έργο i-DREAMS, εύρος ανοχής ασφαλείας, μεθοδολογία χαρτογράφησης, δείκτες κινδύνου, πρόβλεψη σε πραγματικό χρόνο.*

# 1. INTRODUCTION

The overall objective of the European H2020 i-DREAMS[1] project is to define, develop, test and validate a context-aware safety envelope for driving in a 'Safety Tolerance Zone' (STZ), with a smart Driver, Vehicle & Environment Assessment and Monitoring System. Taking into account, on the one hand, driver background factors and real-time risk indicators, and on the other hand, driving task complexity indicators, a continuous real-time assessment will be created to monitor and determine if a driver is within acceptable boundaries of safe operation (i.e. Safety Tolerance Zone). Testing and validation will be applied to car, bus and truck drivers as well as to tram and train drivers.

Within a transport system, a driver can be regarded as a human operator (technology assisted) self-regulating control over transportation vehicles in the context of crash avoidance. The concept of the STZ within the i-DREAMS platform attempts to describe short of the range at which self-regulated control is considered safe. It is based on Fuller's Task Capability Interface Model (Ray Fuller, 2000, 2005, 2011) which states that loss of control occurs when the demand of a driving task outweighs the operator's capability.

The STZ contains three phases: normal driving phase, danger phase and avoidable accident phase. Firstly, the normal driving refers to the phase where conditions at that point in time suggest that a crash is unlikely to occur and therefore the crash risk is low and the operator is successfully adjusting their behavior to meet task demands. Fundamental goal of the i-DREAMS platform is to keep drivers within this normal phase. Secondly, the danger phase is characterized by changes to the normal driving that suggest a cash may occur and therefore, there is an increased crash risk. At this stage a crash is not inevitable but becomes more likely. The STZ switches to the danger phase whenever instantaneous measurements detect changes that imply an increased crash risk. Lastly, the switch to avoidable accident phase occurs when a collision scenario is developing but there is still time for the operator to intervene in order to avoid the crash. In this phase, the need for action is more urgent as if there are no changes or corrections in the road or rail traffic system or an evasive manoeuvre is performed by the operator a crash is very likely to occur.

It should be mentioned that the i-DREAMS platform is composed of two modules. The first is the monitoring module that takes measurements relating to the "context" (i.e. environment including infrastructure), "operator" (i.e. driver state and demographic characteristics) and "vehicle" (i.e. technical specifications and current state). These "Context - Operator - Vehicle - COV" measurements are used to infer the demands of the driving task (i.e. task complexity) and the driver's capability to cope with these demands (i.e. coping capacity). These inferences on its turn are used to estimate in which phase within the STZ the driver is operating within at each moment in time. The second module is the in-vehicle intervention module, that is responsible for keeping the driver within the normal phase of the STZ all the times, either by providing a warning or instruction during driving (real-time intervention) or providing information with detailed feedback on the trip as well as improving their performance once the driving task has ended (post-trip intervention). The STZ phase, within which the driver is operating, dictates the type of real-time intervention that is delivered. In the normal driving phase, no intervention is needed. If it is detected that a driver has entered the danger phase, a warning or advice should be given. Entering the avoidable accident phase also requires an intervention, but this may need to be more specific and provide an instruction signal, which impels the operator to take a decisive action.

The conceptual state of the STZ changes dynamically depending upon changes in the driving conditions or system of which the operator is an integral part. The drivers' self-regulated control has many influences, one of which is the driver's own perception of the driving conditions. Drivers seek to maintain a level of risk that they are comfortable with and continuously adapt their behavior to achieve the subject to a complex network of underlying motivations, not all of which relate to safety. This implies that drivers may choose to intentionally behave in a way that objectively would be considered unsafe (i.e. travelling close to a vehicle ahead). A driver's subjective appraisal of risk does not necessarily therefore correspond to that calculated with objective measures, nevertheless the driver would still be classed as operating within the danger or avoidable accident phases of the STZ (Ray Fuller, 2011).

It is worth mentioning that data analysis consists a pivotal part of this project for achieving its objectives and the methods for data analysis highly depend on the collected data. In order to model the STZ, the available data as well as the potential outcome of the model need to be considered. For suggesting a positive outcome, the data to be used as input for the model will be available in real-time, as the measurements of task demand (e.g. road layout, weather conditions, time of the day) and coping capacity (e.g. fatigue, distraction, sleepiness) are going to be sequential. Furthermore, as the STZ is the "trigger" for real-time and post-trip interventions, the algorithm outputs are required also to be provided online as in real-time and hence both dynamic and static modelling approaches need to be considered. Distinguishing between the three levels of STZ (i.e. normal driving, danger and avoidable accident phases) in real-time, turns STZ modelling into a ternary classification problem, where raw measurements need to be classified as belonging to one of the three existing levels. This classification problem however implies that the feed to the training part of these algorithms needs to be conveniently labelled.

[1] Further general project information can be found on the website: **https://idreamsproject.eu**

Within, the above framework, the aim of the current study is to provide guidelines for mapping the concept of the STZ using continuous outcome variables. The overall objective is to further elaborate on the analytical methods and modelling options, their strengths, limitations and applications in i-DREAMS. Particular focus will be given in continuous variables of risk and the most reliable indicators are going to be investigated in real-time. For instance, time headway, speed, acceleration, deceleration, distraction, fatigue or sleepiness consist some of the continuous variables in order to model the concept of the i-DREAMS project.

The paper is structured as follows. In the beginning, the overall objective of the i-DREAMS project as well as the aim of this research is provided. Subsequently, a thorough literature review of models dealing with driver behavior and collision risk modelling in real-time are provided. Then, the most prominent approaches are detailed analyzed and a brief description of their underpinning procedure is given. Additionally, initial insights into analyses and results for real-time purposes are presented. Lastly, overall conclusions as well as practical considerations concerning the modelling of the STZ are highlighted in order to assist researchers and practitioners.

# 2. BACKGROUND

Predicting driving behavior by employing mathematical driver models, obtained directly from the observed driving-behavior data, has gained much attention in literature (Girma et al., 2019; Kanaan et al., 2019; McDonald et al., 2019; Xue et al., 2019; Zou et al., 2018). Several models have been used to address road safety and the estimation of driving behavior, many of which in the context of experimental studies, including driving simulator studies and field operational trials and/or naturalistic driving studies. The aim of this section is to examine different models as well as methodologies that include the relationship and interaction between task demand and coping capacity. both static and dynamic state-of-the-art approaches that could be employed to convert driving behavior data into meaningful STZ information are reviewed. The most suitable models, able to estimate driving behavior and crash risk will be employed for the scope of the i-DREAMS project. Literature was searched within popular scientific databases such as Scopus, ScienceDirect and Google Scholar. All studies were screened on the basis of their title and abstract in order to select the studies presented in the following review.

## 2.1 Bayesian Networks

In recent years, BNs have been quite popular in modelling massive amounts of data with the need for data aggregation and model flexibility (Li et al., 2014; Tandon et al., 2016). Lefθvre et al. (2012) proposed a DBN which focused on intersection accidents caused by driver errors. Their approach was formulated as an inference problem where intention and expectation were estimated jointly for the vehicles converging to the same intersection and the proposed solution was validated by field experiments using passenger vehicles. The results demonstrated the ability of the algorithm to issue a warning in dangerous situations, and the benefits of taking into account interactions between the vehicles when reasoning about situations and risk at road intersections. The use of the Bayesian formalism allowed to take into account uncertainties on the relationships between the variables. The intuitive formulation of risk provided the required flexibility for safety applications relevant to both ADAS and autonomous driving. However, information about drivers' actions, such as steering angle and pedal pressure were not taken into account.

In addition, Zhu et al. (2017) utilized a hierarchical BN model to investigate the relationship between observed vehicle motion and a driver's historical crash involvements through the hidden layers of driving behavior and crash risk. The results suggested that the contextual model performs significantly better than the non-contextual model. The method was also effective in handling massive trajectory data and flexible in the data aggregation process. However, the contextual indicators have been more comprehensive by including more variables beyond current roadway type, traffic and relative speeds.

Katrakazas et al. (2019) developed a new risk assessment methodology that integrates a collision risk network-level (CRN) with collision risk vehicle-level (CRV) estimates in real-time under the joint framework of interaction-aware motion models and DBN. Results indicated an enhancement of the interaction-aware model by up to 10%, when traffic conditions were deemed as collision-prone. The network-level collision information could assist not only the identification of "dangerous" road users but also act as a safety net for all the motion planning levels and is suitable for Connected and Autonomous Vehicles (CAVs). It is however noteworthy that the extracted probabilities for all the scenarios were not sufficiently high and the scenarios were built on some assumptions and without highly detailed vehicle-level data.

The work by Shankar et al. (2008) pointed out that hierarchical DBN can be used to reflect how driver decisions are made: driver-level predictors, such as years of driving, can be used to parameterize the effects of event attributes and context. There were found some advantages related to parameter uncertainty, sample specificity and extensibility to large data sets, which can capture driver differences over time and space, but non automated storage of data through the DAS with a flag for potential risk was identified.

## 2.2 Clustering Models

Clustering techniques have been used by researchers to categorize drivers who are compliant and non-compliant. Xue et al. (2019) developed a driving style recognition method (safe, low-risk, high-risk, dangerous) based on vehicle trajectories from video recordings and k-means clustering, failing however to take into account road conditions and traffic flow levels. An individually-tailored, real-time feedback-reward system for in-vehicle interventions was installed in driver's own vehicles and its effect was researched in a field trial with 37 participants by Merrikhpour et al. (2014). Drivers were clustered by compliance rate, pre and post interventions, in more speed and headway compliant and less speed and headway compliant and the results showed that speed limit and headway compliance increased with post-intervention in the non-compliant group. However, it is not clear if the observed benefits were due to either feedback, or reward, or the unique combination of both. The

study by Wang and Xu (2019) using SHRP2 data followed a two-level approach; first, a K-means algorithm was adopted to classify drivers into groups of high, moderate or low risk level and second, logistic regression models for each risk group indicated the probability of each driver getting involved in an incident. Drivers themselves participated in this study by validating any traffic event using an in-vehicle event button and by self-assessing their behavior due to inattention and inexperience errors.

### 2.3 Fuzzy Logic Models

Machine learning techniques have been used in primarily traffic flow modelling and second in road safety analysis. Imkamon et al. (2008) proposed a new Fuzzy Logic inference system which can record driving events, detect unsafe or risk driving behavior and classify levels of hazardous driving by employing data from sensors that measure three different perspectives (an ECU reader, an accelerometer, and a camera). The test results showed that the system can perform well compared with human opinions. However, the current system had a limitation of day-time operation due to constraints. In addition, Chong et al. (2013) trained a fuzzy rule-based neural network to model the acceleration of a car-following vehicle. Fuzzy logic was used to discretize traffic state and action variables and reinforcement learning was used for the neural network to learn driving behavior from naturalistic data. On the one hand this paper showcased the application of fuzzy rules on continuous variables with high R-squared values, but on the other hand the choice of model parameters and the number of car-following events were limited (ten in total). Fuzzy deep learning was also applied for traffic incident detection (El Hatri and Boumhidi, 2018), where the authors performed a comparison of machine learning models based on MSE with detection rate and mean time to detection as criteria. Their implementations showcased a high detection rate, low false alarm rate and a back-propagation feature to adjust the parameters in the deep network, although model validation was done on highly artificial street network and incident occurrences. The standard deviation of detection time was not given, indicating questionable potential for applying this algorithm.

### 2.4 Hybrid Input Output Automaton

According to Bouhoute et al. (2014), a Hybrid Input Output Automaton (HIOA) is a formal model that used to describe discrete and continuous behavior of a system. A driver-centric approach to model risky driving behavior in vehicular ad hoc networks was proposed. Their advantage consisted of providing a better analysis of hybrid systems. The constructed automaton corresponded to the supposed behavior of the driver in one trip, exploration of other states possible in next trips. The goal of the proposed example was to illustrate the idea of the modelling approach and how it can be applied. Consequently, despite the constructed model may be useful to predict the driver behavior in the future, prevent unsafe situations and provide more comfort to the driver, the implementation of the model and the learning process have been not implemented yet.

### 2.5 Long Short-Term Memory Models

Girma et al. (2019) proposed deep learning-based models, called LSTM models, to predict and identify drivers based on their individual's unique driving patterns based on vehicle telematics data. Results showed that the proposed model prediction accuracy remained satisfactory and outperformed other approaches despite the extent of anomalies induced in the data. Even under increasing noise and outliers' effect, the proposed approach maintained its accuracy above the acceptable value, 88%, while other models' accuracy fell below 40%. Neural network-based models such as LSTM performed better than Fully Connected Neural Network (FCNN), Decision Tree (DT) or RF, by avoiding over-fitting on the noise. Bao et al. (2019) trained a spatiotemporal convolutional LSTM network to determine a crash risk scale and to calibrate a crash risk alarm threshold. Their data comprised large-scale taxi GPS data, population data, weather and land use features, and they were used to compare econometric and machine learning models. Econometric models performed better than machine-learning models in weekly crash risk prediction tasks, while they exhibit worse results than machine-learning models in daily crash risk prediction tasks. However, because taxi trips were not representative of the general mobility patterns in a city, this study entails a significant sample bias problem.

### 2.6 Recommendation

With regards to safety and risk level, several models and methodologies have been examined. From the aforementioned approaches examined, DBNs were found to be the most effective and extensible in handling massive trajectory data, as well as flexible for safety applications in the data aggregation process (Lefθvre et al., 2012; Shankar et al., 2008; Zhu et al., 2017). The use of the Bayesian formalism allowed to take into account uncertainties on the relationships between the variables (Lefθvre et al., 2012). However, variable selection, assumptions and non-highly detailed vehicle-level data were found to be some of the shortcomings of this approach (Katrakazas et al., 2019). Lastly, LSTMs revealed the highest accuracy, compared with other models examined. Specifically, the proposed model maintained its accuracy above the acceptable value 88%, while other models' accuracy fell below 40%. LSTM had an inherent ability to remember temporal information in data and conserve it for many time steps, unlike other conventional machine learning approaches (Girma et al., 2019).

## 3. METHODOLOGICAL OVERVIEW

According to the research question and hypothesis made, a mapping exercise of machine learning algorithms was implemented for real-time data prediction. It should be noted that the fundamental research question within the i-DREAMS project is how explanatory variables (i.e. various indicators of task complexity and coping capacity) are correlated with the dependent variable "risk".

A variety of analytical methods and potential modelling approaches has been reviewed, among which two methods have been selected to be used in i-DREAMS: Dynamic Bayesian Networks (DBN) and Long Short-Term Memory (LSTM) deep neural networks. Each of these two methods has strengths and limitations, making it suitable for a certain purpose in the project. Based on the methodological background, an attempt was made to transform the model approach into a suitable structure which will allow to response to the research question made. The key output is expected to be the correlation of

the explanatory variables and various indicators of task complexity and coping capacity with the dependent variable risk.

### 3.1 Dynamic Bayesian Network analytical approach

It is hypothesized that a situation is risky if the level of task complexity is different from the level of coping capacity. For example, if the driving is task is difficult and the operator state is decreased, then risk is probable. In order to identify risk, the level of task complexity as well as the level of coping capacity need to be predicted and compared. As a result, the hypothesis forms a real-time multi-level classification problem, where the dependent variable takes the form of a category representing the difference of task complexity and coping capacity. Task Complexity variables (X1) and coping capacity variables (X2) can be used to identify individual levels of coping capacity and task complexity, and can also be supplemented by other indicators to predict Y. The relationship between the variables and their causal relationship can be depicted in the following flowchart in Figure 1

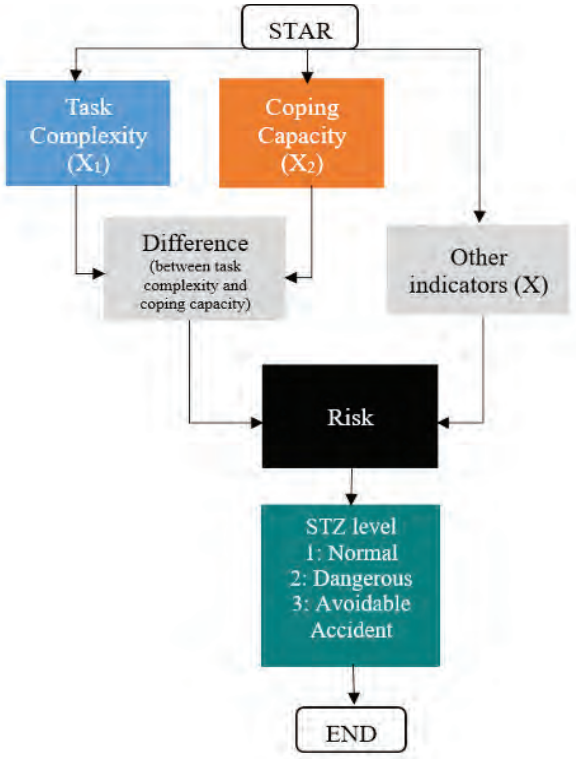


**Figure 1: The causal relationship between the variables of task complexity and coping capacity**

With regards to the model specification, the raw sensor measurements will be observed. By filtering these raw measurements, the COV indicators will become available, so they will be used to determine the coping capacity and task complexity at each time moment. Hence, the two layers of coping capacity and task complexity depend on the COV indicators. Finally, as the operator's capacity indicates the ability of the driver to operate safely with regards to the task imposed, the operator's capacity depends on the complexity of the task. The proposed DBN structure along with the proposed characteristics to estimate task complexity and coping capacity is depicted in Figure 2.

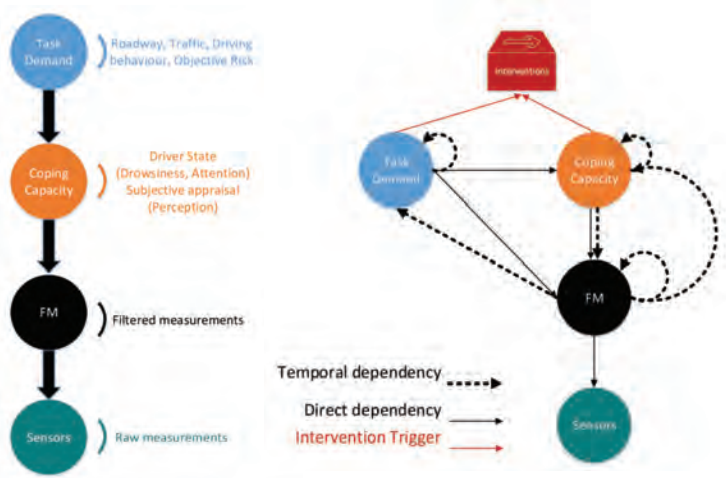


**Figure 2: The proposed DBN for STZ modelling**

The proposed DBN can be described by the joint distribution:

$$P(TC^{0:T}, CC^{0:T}, FM^{0:T}, Z^{0:T}) = P(TC_0, CC_0, FM_0, Z_0) \prod_{t=1}^{T} P(TC_t|TC_{t-1}FM_{t-1})\, P(CC_t|TC_tCC_{t-1}FM_{t-1}) \quad (1)$$
$$t \in \mathbb{N} \text{ and } t \leq T$$

where:

- TC: Task Complexity
- CC: Coping Capacity
- FM: Filtered COV Measurements
- Z: Raw measurements
- t: current time step
- T: Total time of measurements

The expected task complexity $P(CC_t|TC_tCC_{t-1}FM_{t-1})$ is derived from the previous task complexity and the available indicators on environment variables (i.e. time of day, wipers on/off, low visibility indicator, road environment, road geometric configuration and traffic density).

$$P(TC_t|TC_{t-1}FM_{t-1}) = f(Environment, Vehicle\ variables, TC_{t-1}) \quad (2)$$

Coping capacity $P(CC_t|TC_tCC_{t-1}FM_{t-1})$ can be estimated through functions that correlate the effect of task complexity on coping capacity (Faure et al., 2016) modified by a factor to take the previous coping capacity into account.

$$P(CC_t|TC_tCC_{t-1}FM_{t-1}) = f(Driver,\ TC_t, CC_{t-1}) \quad (3)$$

The filtered measurements $P(FM_t|FM_{t-1}TC_tCC_tCC_{t-1})$ is the probability of the indicator values based on the current task complexity and coping capacity as well as their previous values and the previous coping capacity can be mapped based on the specific scenarios that will be tested in the simulators. In that way, specific ranges of values or task complexity - and coping capacity-specific measurements along with their corresponding probabilities of appearance can be identified.

For the probability of the raw measurements $P(Z_t|FM_t)$ a sensor model based on Agamennoni et al. (2011) and the Student t-distribution can be followed. In order to identify the different STZ levels, a comparison between the layers of task complexity and coping capacity will be made. The following probability is proposed to be inferred in order to identify avoidable accident or dangerous STZ levels. It should be mentioned that this probability refers to situations that task complexity and coping capacity are beyond normal operations (i.e. increased or high task complexity with decreased or low coping capacity) given the available sensor observations.

$$P(TC \neq normal \cup CC \neq normal \mid Sensors) \quad (4)$$

Examples of the different STZ levels according to task complexity and coping capacity are highlighted in Table 1. It can be observed that low coping capacity leads to avoidable accident or dangerous phase, decreased coping capacity leads to dangerous or normal phase, while high coping capacity leads to Normal phase, regardless the other layers of task complexity.

**Table 1: Different STZ levels according to task complexity and coping capacity**

| Task Complexity | Coping Capacity | STZ Level |
|---|---|---|
| High | Low | Avoidable Accide |
| High | Decreased | Dangerous |
| High | High | Normal |
| Increased | Low | Avoidable Accide |
| Increased | Decreased | Dangerous |
| Increased | High | Normal |
| Low | Low | Dangerous |
| Low | Decreased | Normal |
| Low | High | Normal |

The likelihood function for Bayesian Networks is the same as in the frequentist inference. More specifically,

$$likelihoodi = \pi(xi)^{yi}(1-\pi(xi))^{(1-yi)} \quad (5)$$

where:

- $xi$ is the covariate vector
- $\pi(xi)$ is the probability of the event for the $i^{th}$ subject which has covariate vector $xi$
- $yi$ is the multiple dependent variable representing the risk probability which has the outcomes y=0 (STZ: Normal Phase), y=1 (STZ: Dangerous Phase) and y=2 (STZ: Avoidable Accident Phase)

The logistic regression equation is:

$$\log\left(\frac{p}{1-p}\right) = \beta_0 + \beta_1 x_1 + \cdots + \beta_n x_n \quad (6)$$

where:

- $\beta_0$ is the intercept
- $\beta i$ is a coefficient for the explanatory variable $xi$

In addition, similarly to the frequentist approach, taking the exp(β) provides the odds ratio for one unit change of that parameter.

## 3.2 Long Short-Term Memory analytical approach

With regards to the modelling approach, it is assumed that there is a specific risk factor (i.e. task complexity or coping capacity) along with the corresponding measurements and metrics for each variable. At each time, a specific risk factor (i.e. STZ levels of each risk factor are known) is targeted but other important variables (e.g. weather conditions, distraction, etc.) can also be used in the same model in order to make the prediction. The entire dataset will be split into train and test set. Based on these indicators, there is a need to predict the risk, and therefore, the time spent in each STZ level (i.e. normal, dangerous, avoidable accident). The problem is a real-time regression problem and can be solved by the LSTM formulation. In order to make sure that the risk calculated is reliable, a good level of forecast accuracy for all the STZ levels should be performed. For instance, if a good prediction for the "avoidable accident" phase can be produced, it should be made clear that a good prediction for the "normal" phase, can be produced as well. This implies that the level of the STZ should be known beforehand, otherwise this hypothesis needs to be supplemented by a classification problem or a clustering one. The flowchart associated with this hypothesis is shown in Figure 3.

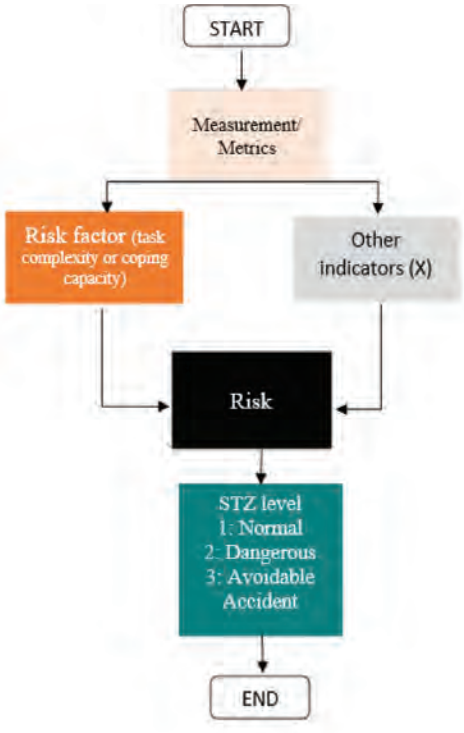


**Figure 3: The proposed LSTM for STZ modelling**

With regards to the second proposed LSTM model, the problem of defining the STZ levels becomes more straightforward, since LSTMs as a sub-category of Deep Neural Networks act like "black-boxes" (Xu et al., 2013) and thus the only input that needs to be provided to the model are labelled time series data. The proposed approach using LSTMs is given in Figure 4.

In the proposed solution with LSTMs, historical sensor data will be used to extract and select features of the measurements to obtain the most important for STZ level detection. Afterwards, the most important measurements for monitoring the environment the

vehicle and the driver become the input to an unsupervised learning algorithm that will group together measurements according to task demand and coping capacity, which, in turn, will act as input for training the LSTM model. After training the LSTM model with the labelled time-series data, the available real-time sensor data will be used as input for the model to predict the STZ level in the subsequent time.

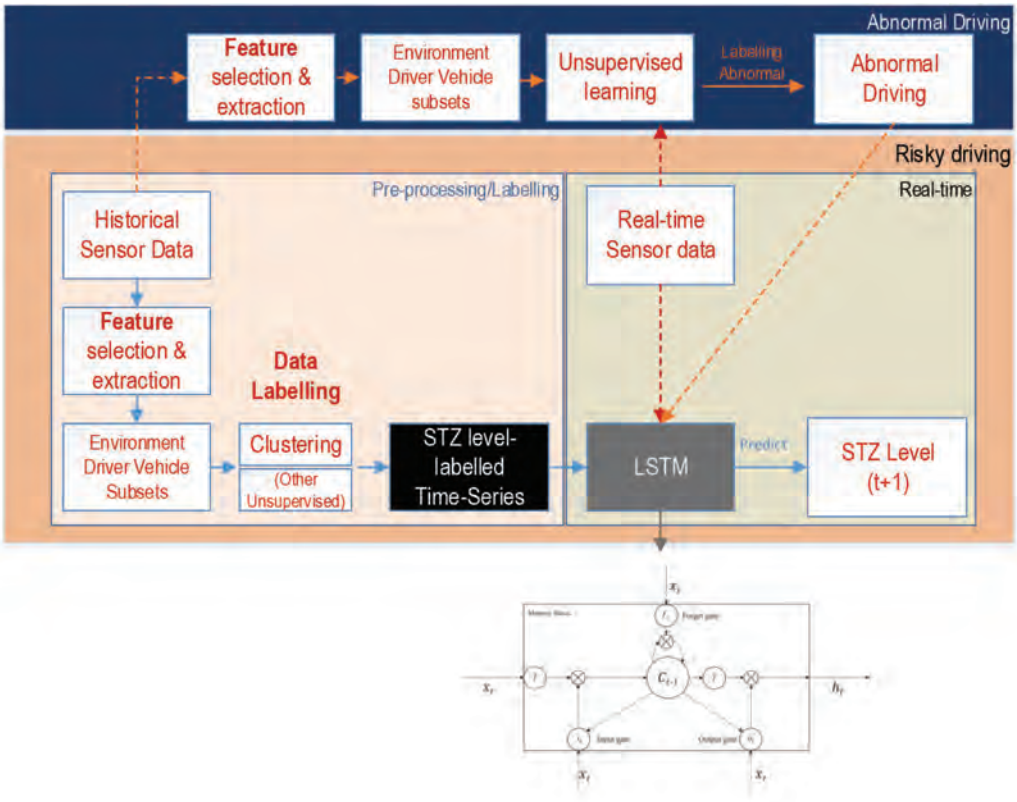


**Figure 4: STZ modelling using LSTMs**

## 4. RESULTS

In order to model the concept of the i-DREAMS project several parameters were examined. Particular emphasis was given to average speed and a new variable was created taking into account the different levels of STZ. Thus, the dependent variable was the STZ_speed which was divided into three levels (i.e. normal phase:0, dangerous phase: 1, avoidable accident phase: 2). Then, the correlation of the independent variables (i.e. TTC – time to collision with vehicle ahead, Headway - time headway to vehicle ahead in same lane, Distance travelled - distance driving, HandsOnEvent - whether hands are on the steering wheel, FatigueEvent - KSS score, ME_ForwardCollisionWarning - whether forward collision warning is active and ME_LaneDepartureWarningActive - whether lane departure warning is active) was investigated. No strong correlation among these indicators was identified, as shown in Table 2.

**Table 2: Correlation of independent variables**

| | Headway | TTC | Distance.travelled | HandsOnEvent | FatigueEvent | ME_ForwardCollision Warning | ME_LaneDeparture WarningActive |
|---|---|---|---|---|---|---|---|
| **Headway** | 1,000 | 0,000 | -0,081 | -0,098 | -0,124 | -0,005 | -0,024 |
| **TTC** | 0,000 | 1,000 | 0,000 | -0,010 | -0,078 | 0,001 | -0,007 |
| **Distance.travelled** | -0,081 | 0,000 | 1,000 | 0,024 | 0,097 | 0,004 | 0,000 |
| **HandsOnEvent** | -0,098 | -0,010 | 0,024 | 1,000 | | | |
| **FatigueEvent** | -0,124 | -0,078 | 0,097 | | 1,000 | | |
| **ME_ForwardCollision Warning** | -0,005 | 0,001 | 0,004 | | | 1,000 | -0,008 |
| **ME_LaneDeparture WarningActive** | -0,024 | -0,007 | 0,000 | | | -0,008 | 1,000 |

A feature importance algorithm extracted from XGBoost was used in order to evaluate the significance of variables on forecasting STZ and select the most appropriate independent variables. Headway, distance travelled and TTC were the most important factors of all examined indicators, while the parameters of forward collision warning and lane departure warning active were less significant. Table 3 provides the feature importance of independent variables based on XGBoost algorithm implemented.

**Table 3: Feature importance of independent variables**

| | Variables | Importance |
|---|---|---|
| 1 | Headway | 0.4628857977881 |
| 2 | Distance.travelled | 0.3689770387145 |
| 3 | TTC | 0.1681097785940 |
| 4 | ME_ForwardCollisionWarning | 0.0000203474815 |
| 5 | ME_LaneDepartureWarningActive | 0.0000004199277 |

A short dataset of 10,000 rows was used and a Neural Network model was implemented. As presented in Figure 5, in this study, there are three neurons in the input layer (i.e. headway, distance.travelled, TTC) and one neuron in the output layer (STZ).

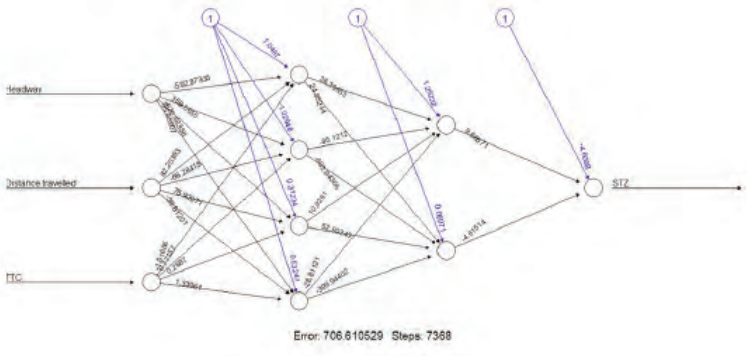


**Figure 5: The multi-layer Neural Network model layout for STZ**

Then, a table of confusion which contains two rows and two columns that reports the number of false positives, false negatives, true positives, and true negatives was created. This allows more detailed analysis than mere proportion of correct classifications (e.g. accuracy). In particular, negative class refers to the Normal phase, positive class refers to the Dangerous phase, while no instances for Avoidable Accident Phase were detected, as shown in Table 4.

**Table 4: Confusion data matrix**

| | Predicted Class | |
|---|---|---|
| Actual (True) Class | 0 | 1 |
| 0 | True Negative (TN) **157** | False Positive (FP) **797** |
| 1 | False Negative (FN) **0** | True Positive (TP) **1546** |

With regards to the assessment of classification model, average classification accuracy represents the proportion of correctly classified observations, while precision, recall and specificity, which are three major performance metrics, describe a predictive classification model. F1-score is calculated in order to find a balance between precision and recall. The geometric mean G-mean is a product of the prediction accuracies for both classes, i.e recall: accuracy on the positive examples, and specificity: accuracy on the negative examples. Lastly, the false positive rate refers to the expectancy of the false positive ratio (i.e. the probability of falsely rejecting the null hypothesis for a particular test). Table 5 provides the assessment of classification model.

**Table 5: Assessment of classification model**

| Accuracy | Precision | Recall | Specificity | f1-score | G-Means | FP Rate |
|---|---|---|---|---|---|---|
| 0,68 | 0,66 | 1 | 0,16 | 0,80 | 0,81 | 0,84 |

## 5. CONCLUSIONS

Following a thorough literature review of models dealing with driver behavior and collision risk modelling in real-time, the most prominent approaches were found to be Dynamic Bayesian Networks or DBNs (a probabilistic graphical time-series model) and Long Short-Term Memory networks or LSTMs (a deep neural network formulation). These two dynamic approaches were chosen due to their efficiency and flexibility in real-time predictions and were found to be suitable for prediction of continuous indicators of risk (e.g. fatigue, speed, time headway, distraction, harsh acceleration). Such a continuous indicator of risk may be the result of combining discrete indicators of risk for different risk factors (which will help validate STZ) or may be the time that is spent in each phase of STZ (which will help tuning the frequency/pitch/presentation of warnings).

While the review of the analytical methods presented previously provided a good understanding of the potential modelling candidates in i-DREAMS and the final selected methods seem plausible, there are still some open issues that need to be considered for model selection. For example, the suggested methods may be confronted with additional limitations considering the ongoing discussions on the different types of data being collected in i-DREAMS. In addition, a number of new limitations have been identified with additional deeper investigations into these methods. For example, it is noted that LSTM is not able to incorporate the inter-relationship between variables into real-time predictions.

Preliminary results indicated a strong relationship between STZ and the independents variables of headway, distance.travelled and TTC. However, it should be highlighted that when more data are available, the most crucial risk indicators of task demand and coping capacity will be extracted and the initial hypothesis described in the paper will be confirmed.

**6. References**


- Agamennoni, G., Nieto, J. I., & Nebot, E. M. (2011). A Bayesian approach for driving behavior inference. In 2011 IEEE Intelligent Vehicles Symposium (IV) (pp. 595-600). IEEE.
- Bao, J., Liu, P., & Ukkusuri, S. V. (2019). A spatiotemporal deep learning approach for citywide short-term crash risk prediction with multi-source data. Accident Analysis & Prevention, 122, 239-254.
- Bouhoute, A., Berrada, I., & El Kamili, M. (2014). A formal model of human driving behavior in vehicular networks. In 2014 International Wireless Communications and Mobile Computing Conference (IWCMC) (pp. 231-236). IEEE.
- Chong, L., Abbas, M. M., Flintsch, A. M., & Higgs, B. (2013). A rule-based neural network approach to model driver naturalistic behavior in traffic. Transportation Research Part C: Emerging Technologies, 32, 207-223.
- El Hatri, C., & Boumhidi, J. (2018). Fuzzy deep learning based urban traffic incident detection. Cognitive Systems Research, 50, 206-213.
- Girma, A., Yan, X., & Homaifar, A. (2019). Driver identification based on vehicle telematics data using LSTM-recurrent neural network. In 2019 IEEE 31st International Conference on Tools with Artificial Intelligence (ICTAI) (pp. 894-902). IEEE.
- Imkamon, T., Saensom, P., Tangamchit, P., & Pongpaibool, P. (2008). Detection of hazardous driving behavior using fuzzy logic. In 2008 5th International Conference on Electrical Engineering/Electronics, Computer, Telecommunications and Information Technology (Vol. 2, pp. 657-660). IEEE.
- Kanaan, D., Ayas, S., Donmez, B., Risteska, M., & Chakraborty, J. (2019). Using Naturalistic Vehicle-Based Data to Predict Distraction and Environmental Demand. International Journal of Mobile Human Computer Interaction (IJMHCI), 11(3), 59-70.
- Katrakazas, C., Quddus, M., & Chen, W. H. (2019). A new integrated collision risk assessment methodology for autonomous vehicles. Accident Analysis & Prevention, 127, 61-79.
- Lefevre, S., Laugier, C., & Ibapez-Guzman, J. (2012, June). Risk assessment at road intersections: Comparing intention and expectation. In 2012 IEEE Intelligent Vehicles Symposium (pp. 165-171). IEEE.
- Li, M., Liu, J., Li, J., & Kim, B. U. (2014). Bayesian modeling of multi-state hierarchical systems with multi-level information aggregation. Reliability Engineering & System Safety, 124, 158-164.
- McDonald, A. D., Ferris, T. K., & Wiener, T. A. (2020). Classification of driver distraction: A comprehensive analysis of feature generation, machine learning, and input measures. Human factors, 62(6), 1019-1035.
- Merrikhpour, M., Donmez, B., & Battista, V. (2014). A field operational trial evaluating a feedback–reward system on speeding and tailgating behaviors. Transportation research part F: traffic psychology and behaviour, 27, 56-68.
- Fuller, R. (2000). The task-capability interface model of the driving process. Recherche - Transports - Sıcurıtı, 66, 47–57.
- Fuller, R. (2005). Towards a general theory of driver behaviour. Accident analysis & prevention, 37(3), 461-472.
- Fuller, R. (2011). Driver control theory: From task difficulty homeostasis to risk allostasis. In Handbook of traffic psychology (pp. 13-26). Academic Press.
- Shankar, V., Jovanis, P. P., Aguero-Valverde, J., & Gross, F. (2008). Analysis of naturalistic driving data: prospective view on methodological paradigms. Transportation research record, 2061(1), 1-8.
- Tandon, P., Huggins, P., Maclachlan, R., Dubrawski, A., Nelson, K., & Labov, S. (2016). Detection of radioactive sources in urban scenes using Bayesian Aggregation of data from mobile spectrometers. Information Systems, 57, 195-206.
- Wang, X., & Xu, X. (2019). Assessing the relationship between self-reported driving behaviors and driver risk using a naturalistic driving study. Accident Analysis & Prevention, 128, 8-16.
- Xu, C., Wang, W., & Liu, P. (2012). A genetic programming model for real-time crash prediction on freeways. IEEE Transactions on Intelligent Transportation Systems, 14(2), 574-586.
- Xue, Q., Wang, K., Lu, J. J., & Liu, Y. (2019). Rapid driving style recognition in car-following using machine learning and vehicle trajectory data. Journal of advanced transportation, 2019.
- Zhu, X., Yuan, Y., Hu, X., Chiu, Y. C., & Ma, Y. L. (2017). A Bayesian Network model for contextual versus non-contextual driving behavior assessment. Transportation research part C: emerging technologies, 81, 172-187.
- Zou, Q., Li, H., & Zhang, R. (2018). Inverse Reinforcement Learning via Neural Network in Driver Behavior Modeling. In 2018 IEEE Intelligent Vehicles Symposium (IV) (pp. 1245-1250). IEEE.



***Eva Michelaraki[1*], Christos Katrakazas[2], Tom Brijs[3], George Yannis[4]***

[1,2,4] National Technical University of Athens,
Department of Transportation Planning and Engineering,
5 Heroon Polytechniou str., GR-15773, Athens, Greece
[3]UHasselt, School of Transportation Sciences
Transportation Research Institute (IMOB),
Agoralaan, 3590 - Diepenbeek, Belgium

Φοιτήτρια | **Αικατερίνη Σκλιάμη**
Επιβλέπων Καθηγητής | **Γεώργιος Γιαννής,** Καθηγητής ΕΜΠ
Εκπαιδευτικό ίδρυμα | **ΕΜΠ - Σχολή Πολιτικών Μηχανικών**
Είδος εργασίας | **Για την απόκτηση Προπτυχιακού Διπλώματος**

# ΣΥΓΚΡΙΤΙΚΗ ΑΝΑΛΥΣΗ ΧΑΡΑΚΤΗΡΙΣΤΙΚΩΝ ΟΔΙΚΩΝ ΑΤΥΧΗΜΑΤΩΝ ΑΝΑ ΕΘΝΙΚΟΤΗΤΑ ΟΔΗΓΟΥ ΣΤΗΝ ΕΥΡΩΠΑΪΚΗ ΕΝΩΣΗ

## Περίληψη Εργασίας

**Στόχος** της παρούσας Διπλωματικής Εργασίας είναι η συγκριτική ανάλυση των χαρακτηριστικών των οδικών ατυχημάτων για τις διαφορετικές εθνικότητες θανόντων οδηγών στην Ευρωπαϊκή Ένωση, με τη χρήση στατιστικών μοντέλων.

Τον καθορισμό του επιδιωκόμενου στόχου ακολούθησε η **βιβλιογραφική ανασκόπηση**, στην οποία αναλύθηκαν τα αποτελέσματα συναφών ερευνών με το αντικείμενο της παρούσας Διπλωματικής Εργασίας, τόσο σε εθνικό, όσο και Ευρωπαϊκό και παγκόσμιο επίπεδο. Για τον αριθμό των θυμάτων από οδικά ατυχήματα, τα στοιχεία αντλήθηκαν από την Ευρωπαϊκή βάση δεδομένων οδικών ατυχημάτων, **CARE**. Ως περίοδος μελέτης ορίστηκε η δεκαετία 2008-2017. Τη συλλογή των δεδομένων ακολούθησε η επεξεργασία και κωδικοποίησή τους ώστε να εισαχθούν στο ειδικό στατιστικό λογισμικό.

Ένας επιπλέον διαχωρισμός που πραγματοποιήθηκε, αφορούσε στα Βόρεια και Νότια κράτη της Ευρωπαϊκής Ένωσης. Για τη στατιστική ανάλυση των στοιχείων επιλέχθηκε η **Αρνητική Διωνυμική Παλινδρόμηση**. Τα τελικά μαθηματικά μοντέλα που προέκυψαν αποτυπώνουν τη συσχέτιση μεταξύ της εξαρτημένης μεταβλητής (αριθμός νεκρών οδηγών) και των παραγόντων που την επηρεάζουν.

Τα **γενικά συμπεράσματα** συνοψίζονται ως εξής:

1. Στα κράτη της Ευρωπαϊκής Ένωσης η **εθνικότητα του οδηγού επηρεάζει στατιστικά σημαντικά τον αριθμό των νεκρών** στα οδικά ατυχήματα, ενδεχομένως διότι οι ξένοι οδηγοί δεν είναι τόσο εξοικειωμένοι με την τοπική κυκλοφορία όσο είναι οι ντόπιοι οδηγοί και πιθανώς προσαρμόζονται δυσκολότερα και κάνουν περισσότερα λάθη.
2. Οι **βασικοί παράγοντες επιρροής** των οδικών ατυχημάτων που διαφοροποιούν τα οδικά ατυχήματα ντόπιων και ξένων οδηγών είναι κατά σειρά σπουδαιότητας το φύλο του οδηγού, ο τύπος της περιοχής του ατυχήματος, ο τύπος του εμπλεκόμενου οχήματος, οι καιρικές συνθήκες και τέλος οι συνθήκες φωτισμού του ατυχήματος.
3. Η επιρροή του **φύλου του οδηγού** στον αριθμό των νεκρών είναι μεγαλύτερη στους ντόπιους οδηγούς από ότι στους ξένους.
4. Η επιρροή του **τύπου της περιοχής του ατυχήματος** στον αριθμό των νεκρών είναι μεγαλύτερη στους ξένους οδηγούς από ότι στους ντόπιους οδηγούς.
5. Οι **καιρικές συνθήκες την ώρα του ατυχήματος** έχουν μεγαλύτερη επιρροή στον αριθμό των νεκρών στους ξένους οδηγούς από ότι στους ντόπιους.
6. Η επιρροή των **συνθηκών φωτισμού την ώρα του ατυχήματος** είναι μεγαλύτερη για τους ξένους οδηγούς από ότι για τους ντόπιους οδηγούς.
7. Η επιρροή του **τύπου του εμπλεκόμενου οχήματος** είναι μεγαλύτερη για τους ξένους οδηγούς σε σχέση με τους ντόπιους οδηγούς. Συγκεκριμένα η χρήση των μηχανοκίνητων δικύκλων επηρεάζει σε μεγαλύτερο βαθμό τους ξένους οδηγούς από ότι τους ντόπιους, πιθανώς διότι οι ξένοι οδηγοί προσαρμόζουν δυσκολότερα την οδήγηση των μοτοσυκλετών στις τοπικές συνθήκες κυκλοφορίας.
8. Η επιρροή της **χρήσης του ποδηλάτου** στον αριθμό των νεκρών είναι μεγαλύτερη για τους ξένους οδηγούς σε σχέση με τους ντόπιους οδηγούς, ενδεχομένως διότι οι ξένοι ποδηλάτες προσαρμόζουν δυσκολότερα την οδήγηση των ποδηλάτων τους στις τοπικές συνθήκες κυκλοφορίας.
9. Αξιοσημείωτο είναι επίσης πως μόνο για τους ξένους οδηγούς στις Βόρειες χώρες οι **συνθήκες κακοκαιρίας** οδηγούν σε αύξηση του αριθμού των νεκρών σε οδικά ατυχήματα συγκριτικά με την καλοκαιρία.
10. Τέλος, συνολικά, η επιρροή της **χρήσης του ποδηλάτου** επηρεάζει λιγότερο τους ντόπιους οδηγούς στα **Νότια κράτη της ΕΕ** σε σχέση τόσο με τους ντόπιους όσο και με τους ξένους οδηγούς στα Βόρεια κράτη της ΕΕ.

**Σύνδεσμος**
https://www.nrso.ntua.gr/geyannis/edu/ad97-aikaterini-skliami-comparative-analysis-of-traffic-accident-factors-per-driver-nationality-in-the-european-union/

Φοιτητής | **Γιώργος Πρίφτης**
Επιβλέπων Καθηγητής | **Γεώργιος Γιαννής,** Καθηγητής ΕΜΠ
Εκπαιδευτικό ίδρυμα | **ΕΜΠ - Σχολή Πολιτικών Μηχανικών**
Είδος εργασίας | **Για την απόκτηση Προπτυχιακού Διπλώματος**

# ΕΡΕΥΝΑ ΑΠΟΔΟΧΗΣ ΤΩΝ ΙΠΤΑΜΕΝΩΝ ΑΥΤΟΝΟΜΩΝ ΟΧΗΜΑΤΩΝ ΣΤΗΝ ΕΛΛΑΔΑ

## Περίληψη Εργασίας

Στόχος της παρούσας Διπλωματικής Εργασίας αποτελεί η **διερεύνηση της αποδοχής των ιπτάμενων αυτόνομων οχημάτων στην Ελλάδα**, καθώς και η **πρόθεση χρήσης** αυτών των οχημάτων, ενώ, παράλληλα, καταγράφηκαν οι απόψεις των Ελλήνων για τα ιπτάμενα αυτόνομα οχήματα και τα πιθανά χαρακτηριστικά τους αλλά και για την τεχνολογική τους συνείδηση.

Για τον σκοπό αυτό αναζητήθηκε βιβλιογραφία σχετική με το αντικείμενο της έρευνας σε διεθνές επίπεδο. Ταυτόχρονα, αποφασίστηκε η συλλογή των απαραίτητων στοιχείων να πραγματοποιηθεί μέσω **ερωτηματολογίου**, στο οποίο συμπεριελήφθησαν δέκα σενάρια σύμφωνα με τη μέθοδο της **δεδηλωμένης προτίμησης** από τα οποία οι ερωτηθέντες έπρεπε να επιλέξουν μεταξύ τριών εναλλακτικών: Ι.Χ., ταξί και ιπτάμενο αυτόνομο όχημα.

Τα **σημαντικότερα συμπεράσματα** που προκύπτουν μετά την ανάλυση των αποτελεσμάτων της εφαρμογής των μαθηματικών μοντέλων συνοψίζονται στα εξής σημεία:

- Οι Έλληνες στην πλειοψηφία τους φαίνεται να διατηρούν μια απόμακρη στάση από την επιλογή χρήσης ταξί για τις μετακινήσεις τους, αλλά **εμφανίζονται θετικοί ως προς τα ιπτάμενα αυτόνομα οχήματα**, όταν αυτά γίνουν φθηνά και ασφαλή. Ειδικότερα, όσο εξοικονομείται χρόνος στις μετακινήσεις η πιθανότητα μελλοντικής επιλογής ιπτάμενων αυτόνομων οχημάτων αυξάνεται και για χαμηλά κόστη ξεπερνάει και εκείνη της επιλογής Ι.Χ.
- Η επιλογή ιπτάμενου αυτόνομου οχήματος εξαρτάται από το **κόστος, τον χρόνο και το επίπεδο άνεσης** που αυτά προσφέρουν, γεγονός που επιβεβαιώνεται και από τη διεθνή βιβλιογραφία για την επιλογή μέσου μετακίνησης. Κυριότερος ανταγωνιστής των ιπτάμενων αυτόνομων οχημάτων φαίνεται να είναι το Ι.Χ. Παρόλα αυτά, όταν ο χρόνος και το κόστος μετακίνησης παραμένουν σε χαμηλά επίπεδα και ταυτόχρονα η άνεση κυμαίνεται σε υψηλά επίπεδα τότε η πιθανότητα χρήσης των ιπτάμενων αυτόνομων οχημάτων ξεπερνά εκείνη της χρήσης Ι.Χ.
- Πολύ σημαντικό ρόλο παίζει η **στάση** που έχουν οι ερωτηθέντες απέναντι στα ιπτάμενα αυτόνομα οχήματα, αφού η συντριπτική πλειοψηφία εκείνων που είχαν θετική άποψη και θεωρούσαν ότι θα χρησιμοποιούσαν ένα ιπτάμενο αυτόνομο όχημα φάνηκε να επιλέγουν πιο συχνά αυτό το μέσο για τις μετακινήσεις τους.
- Ένα μεγάλο μέρος του δείγματος διατηρεί επιφυλακτική στάση απέναντι στην αποδοχή των ιπτάμενων αυτόνομων οχημάτων αφού θεωρεί ότι θα είναι **λιγότερο ασφαλή από τα κοινά οχήματα** της εποχής μας και η πλειοψηφία τους δηλώνει ότι θα περίμενε να αισθανθεί άνετα μέχρι να κάνει χρήση τους.
- Τα στατιστικά μοντέλα έδειξαν ότι όσο σημαντικότερη θεωρούν οι ερωτηθέντες την **άνεση** στις μετακινήσεις τους τόσο μειώνονται οι πιθανότητες να επιλέξουν ένα ιπτάμενο αυτόνομο όχημα έναντι του Ι.Χ. τους.
- Όσο περισσότερο σημαντική θεωρούν οι Έλληνες τη **διάρκεια** στις μετακινήσεις τους τόσο αυξάνονται οι πιθανότητες να επιλέξουν ένα ιπτάμενο αυτόνομο όχημα για αυτές, καταδεικνύοντας ότι τα ιπτάμενα αυτόνομα οχήματα ίσως να συμβάλουν σημαντικά στη μείωση της διάρκειας των μετακινήσεών τους.
- Οι Έλληνες που φαίνεται να είναι πιο ψυχροί απέναντι στις δυνατότητες που προφέρονται από τις **νέες τεχνολογίες** και δεν ενθουσιάζονται εύκολα από αυτές ή είναι αδιάφοροι για αυτές, εμφανίζουν σημαντικά μειωμένες πιθανότητες να επιλέξουν ένα ιπτάμενο αυτόνομο όχημα για τις μετακινήσεις τους.
- Αντίστοιχα, **όσοι χρησιμοποιούν νέα τεχνολογικά προϊόντα**, παρόλο το υψηλό κόστος τους και δείχνουν εμπιστοσύνη στην τεχνολογία θεωρώντας πως προσφέρει περισσότερες λύσεις στην καθημερινότητα του ανθρώπου από ότι προβλήματα έχουν περισσότερες πιθανότητες να χρησιμοποιήσουν ιπτάμενο αυτόνομο όχημα.
- Οι **μεγαλύτεροι των 55 ετών δηλώνουν χαμηλότερη προτίμηση στα ιπτάμενα αυτόνομα οχήματα** ενώ οι νεότεροι (18-24) φαίνονται πολύ πιο θετικοί απέναντι στη χρήση τους.
- Οι ερωτηθέντες που ανήκουν σε **πολυμελείς οικογένειες** έχουν την τάση να **επιλέγουν σπανιότερα στις μετακινήσεις τους το ιπτάμενο αυτόνομο όχημα**.
- Το **οικογενειακό εισόδημα** παίζει επίσης ρόλο στην επιλογή των ιπτάμενων αυτόνομων οχημάτων. Συγκεκριμένα, όσων το οικογενειακό εισόδημα κυμαίνεται σε μέσα επίπεδα (10.000-25.000 ευρώ), έχουν περισσότερες πιθανότητες να επιλέξουν ένα ιπτάμενο αυτόνομο όχημα.

**Σύνδεσμος**

https://www.nrso.ntua.gr/geyannis/edu/ad98-george-priftis-investigation-of-flying-autonomous-vehicles-traveller-acceptance-in-greece/

# ΕΠΙΚΑΙΡΑ & ΠΕΡΙΕΚΤΙΚΑ

***Θανάσης Τσιάνος***
Γενικός Γραμματέας ΣΕΣ

**ΜΗΤΡΟΠΟΛΙΤΙΚΟΣ ΦΟΡΕΑΣ** Με μέθοδο και με επιμονή το προηγούμενο χρονικό διάστημα ο ΣΕΣ ενημέρωνε την πολιτεία σχετικά με την αναγκαιότητα της δημιουργίας Μητροπολιτικών Οργανισμών Πολεοδομίας και Μεταφορών (ΜΟ), κατ' αρχήν στις μεγάλες πόλεις της Ελλάδας, μέσω συναντήσεων και κειμένων που αναπτύχθηκαν για τον σκοπό αυτό.

Ως αποτέλεσμα ο Υπουργός Υποδομών και Μεταφορών Κ. Καραμανλής όπως ο ίδιος ανακοίνωσε δημόσια, υιοθετεί την πρόταση του ΣΕΣ για τη δημιουργία ενός ενιαίου φορέα σχετικά με τις μεταφορές στην Αττική. Το όλο εγχείρημα στηρίζει και ο Δήμαρχος Αθηναίων Κ. Μπακογιάννης. Η παραπάνω εξέλιξη είναι ιδιαίτερα σημαντική, δεδομένου ότι ο Μητροπολιτικός Φορέας αποτελεί πάγια θέση του ΣΕΣ τουλάχιστον τα τελευταία 20 χρόνια. Τα μέλη του ΔΣ εκφράζουν την ικανοποίησή τους αφενός που η πρόταση του Μητροπολιτικού Φορέα υιοθετείται από την πολιτεία και αφετέρου αναγνωρίζεται η προσφορά του Συλλόγου.

**ΣΥΓΚΟΙΝΩΝΙΕΣ ΣΤΗΝ ΑΤΤΙΚΗ** Τα κυκλοφοριακά προβλήματα στο Λεκανοπέδιο της Αττικής και η επιστροφή του μέτρου του Δακτυλίου στο κέντρο της Αθήνας, ανέδειξαν σημαντικά συγκοινωνιακά ζητήματα και έφεραν στο επίκεντρο τον Σύλλογο και τα μέλη του. Ο ΣΕΣ με συναίσθηση της μεγάλης ευθύνης του στο να συνεισφέρει στη χώρα μας με επιστημονικά τεκμηριωμένες απόψεις, καθημερινά συνομιλούσε τόσο με τα μέλη του όσο και με την πολιτεία, ενημερώνοντας ταυτόχρονα και την κοινωνία μέσω της συνεχούς παρουσίας του στα Μ.Μ.Ε. τονίζοντας την έλλειψη αλλά και την αναγκαιότητα της εκπόνησης κυκλοφοριακών μελετών στις ελληνικές πόλεις.

Η πολιτεία αναγνωρίζοντας τον θεσμικό επιστημονικό ρόλο και την υπεύθυνη και αντικειμενική στάση του ΣΕΣ, τον καθιστά βασικό συνομιλητή για τη διαμόρφωση του συστήματος μεταφορών στην Αττική σε συνεργασία με όλους τους εμπλεκόμενους φορείς (Υπουργεία – Περιφέρεια – Δήμοι).

**ΠΡΟΩΘΗΣΗ ΘΕΣΕΩΝ ΤΟΥ ΣΕΣ - ΠΡΟΔΙΑΓΡΑΦΕΣ**

Το Δ.Σ. του ΣΕΣ σε κάθε ευκαιρία προωθεί τις θέσεις που ανέπτυξαν οι επιστημονικές επιτροπές του. Επίσης ο ΣΕΣ προωθεί κρίσιμα ζητήματα που σχετίζονται με τη θεσμοθέτηση του ρόλου και του αντικειμένου του συγκοινωνιολόγου, την ανάπτυξη και θεσμοθέτηση προδιαγραφών όπως Γενικών Μελετών Μεταφορών, Κυκλοφοριακών Μελετών, Μελετών Στάθμευσης, Μελετών Κυκλοφοριακών Επιπτώσεων κ.ά. καθώς και αναγκαίες επικαιροποιήσεις / τροποποιήσεις στις υφιστάμενες προδιαγραφές και στην ισχύουσα νομοθεσία. Η ανάπτυξη σύγχρονων, λεπτομερών, ρεαλιστικών και ευέλικτων προδιαγραφών (αντίστοιχων π.χ. με αυτών των υπόλοιπων ευρωπαϊκών κρατών) θα ενδυναμώσει τον ρόλο του συγκοινωνιολόγου και θα αποτελέσει την αναγκαία συνθήκη για τον μετασχηματισμό και τη βελτίωση του συστήματος Μεταφορών στην Ελλάδα.

# ΝΕΑ ΜΕΛΗ

**ΙΩΑΝΝΗΣ ΜΑΤΣΑΣ** εγγράφεται με Α.Μ. 876
**ΠΑΥΛΟΣ ΤΑΦΙΔΗΣ** εγγράφεται με Α.Μ. 877
**ΔΕΣΠΟΙΝΑ ΚΟΥΜΕΝΟΥ** εγγράφεται με Α.Μ. 878
**ΕΛΕΝΗ ΑΝΩΥΡΚΑΤΗ** εγγράφεται με Α.Μ. 879
**ΓΕΩΡΓΙΟΣ ΒΑΓΓΕΛΑΣ** εγγράφεται με Α.Μ. 880
**ΗΛΙΑΣ ΠΑΝΑΓΙΩΤΟΠΟΥΛΟΣ** εγγράφεται με Α.Μ. 881
**ΚΑΛΛΙΡΡΟΗ ΠΟΡΦΥΡΗ** εγγράφεται με Α.Μ. 882
**ΓΙΑΝΝΟΥΛΑ ΤΖΟΒΑΡΑ** εγγράφεται με Α.Μ. 883

# Esri & Autodesk

*GIS & BIM*


## Building Information Modeling - BIM

*Η πρόσφατη και στενή συνεργασία των εταιρειών Esri και Autodesk επικεντρώνεται στη μοντελοποίηση πληροφοριών κτηριακών υποδομών, Building Information Modeling ή BIM. Πρόκειται για ολοκληρωμένα συστήματα πληροφοριών βασιζόμενα σε τεχνικές και διεργασίες υλοποίησης τρισδιάστατων, ευφυών μοντέλων για κτήρια και υποδομές. Παρέχουν στους μηχανικούς που σχεδιάζουν ή κατασκευάζουν τις πάσης φύσεως υποδομές, εκείνες τις τεχνικές και τα εργαλεία για την αποτελεσματική και ολοκληρωμένη μελέτη, σχεδίαση, κατασκευή και διαχείριση υποδομών και κτηρίων.*

### GIS & BIM

***Ο ρόλος των Γεωγραφικών Συστημάτων Πληροφοριών***

Το πολλά υποσχόμενο πεδίο των συστημάτων GIS και BIM προτείνει μία νέα οπτική γωνία στον τρόπο που οι υποδομές, όπως κατοικίες, σχολεία, δρόμοι, δίκτυα κοινής ωφέλειας, σχεδιάζονται και κατασκευάζονται για να εξυπηρετήσουν αποκλειστικά και μόνο το λειτουργικό τους ρόλο. Σύμφωνα με αυτή, οι υποδομές αποτελούν δυναμικό στοιχείο ενός ευρύτερου περιβάλλοντος το οποίο επηρεάζουν, διαμορφώνοντας νέες συνθήκες, οικονομικές, κοινωνικές, περιβάλλοντικές, στα πλαίσια μιας δυναμικής σχέσης.

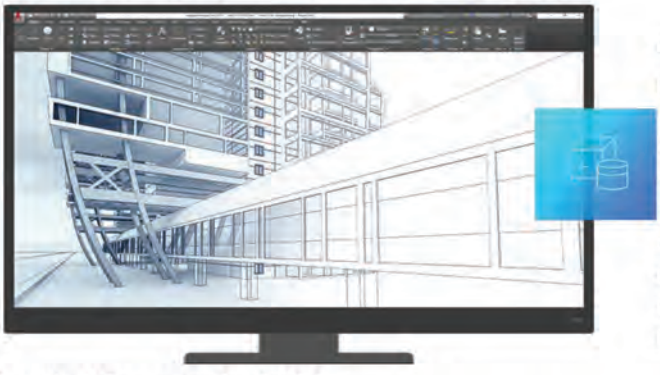

***Διαχείριση δεδομένων σε συστήματα BIM***

Η συμβολή των GIS στην υλοποίηση συστημάτων BIM, επικεντρώνεται πρωτίστως στην διαχείριση δεδομένων. Η συνεργασία Esri και Autodesk δίνει προτεραιότητα στη διαμόρφωση νέων ροών εργασίας που θα διευκολύνουν την ενοποίηση δεδομένων BIM και GIS, ώστε οι χρήστες των συστημάτων τους να τα αξιοποιούν άμεσα και αποτελεσματικά. Επίσης, δίνεται έμφαση στη δυνατότητα ενσωμάτωσης δεδομένων από σύγχρονες πηγές καταγραφής όπως Drones, IoT, 3D models.

**Autodesk Connector for ArcGIS**

Η συνεργασία Esri και Autodesk εξελίσσεται διαρκώς και συστηματικά. Μελετητές και μηχανικοί έχουν ήδη στη διάθεσή τους το προϊόν *Autodesk Connector for ArcGIS*. Από το περιβάλλον του *Autodesk Civil 3D* ή του *InfraWorks* μπορούν να συνδεθούν στο *ArcGIS Online*, εμπλουτίζοντας την εργασία τους με δεδομένα GIS της περιοχής στην οποία το έργο αναπτύσσεται. Αντιστρόφως, από το περιβάλλον *Autodesk Civil 3D* έχουν τη δυνατότητα να προωθήσουν ενημερωμένα δεδομένα του έργου στο *ArcGIS Online για κοινή χρήση*.


# Marathon Data Systems

website: www.marathondata.gr - email: marathon@marathondata.gr - τηλ: 210 6198866

# Όλη η Ελλάδα
# ένας διαλειτουργικός
# αυτοκινητόδρομος


HELLASTRON

Hellenic Association of Toll Road Network

www.hellastron.com